A Multiwavelength Database of Pulsars

Maura Pilia
Alessio Trois
Alberto Pellizzoni

AGILE 13th Workshop – Roma, 25th May 2015

Pulsars..

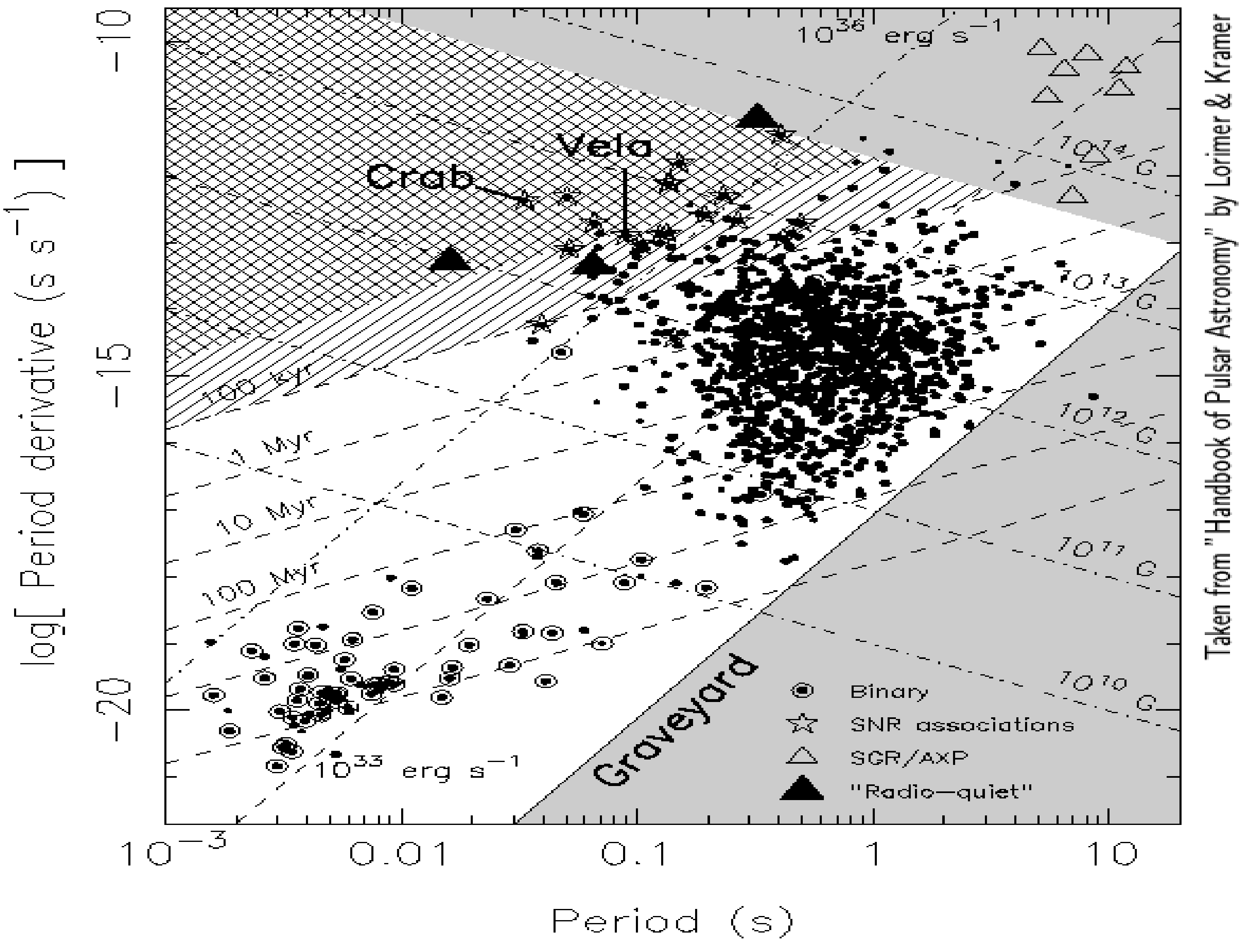

Crab
Vela
10^{36} erg s^{-1}
10^{33} erg s^{-1}
10^{14} G
10^{13} G
10^{12} G
10^{11} G
10^{10} G
100 kyr
1 Myr
10 Myr
100 Myr
Graveyard
Binary
SNR associations
SGR/AXP
"Radio—quiet"
log[Period derivative (s s^{-1})]
−10
−15
−20
10^{-3}
0.01
0.1
1
10
Period (s)
Taken from "Handbook of Pulsar Astronomy" by Lorimer & Kramer

Pulsars in gamma-rays

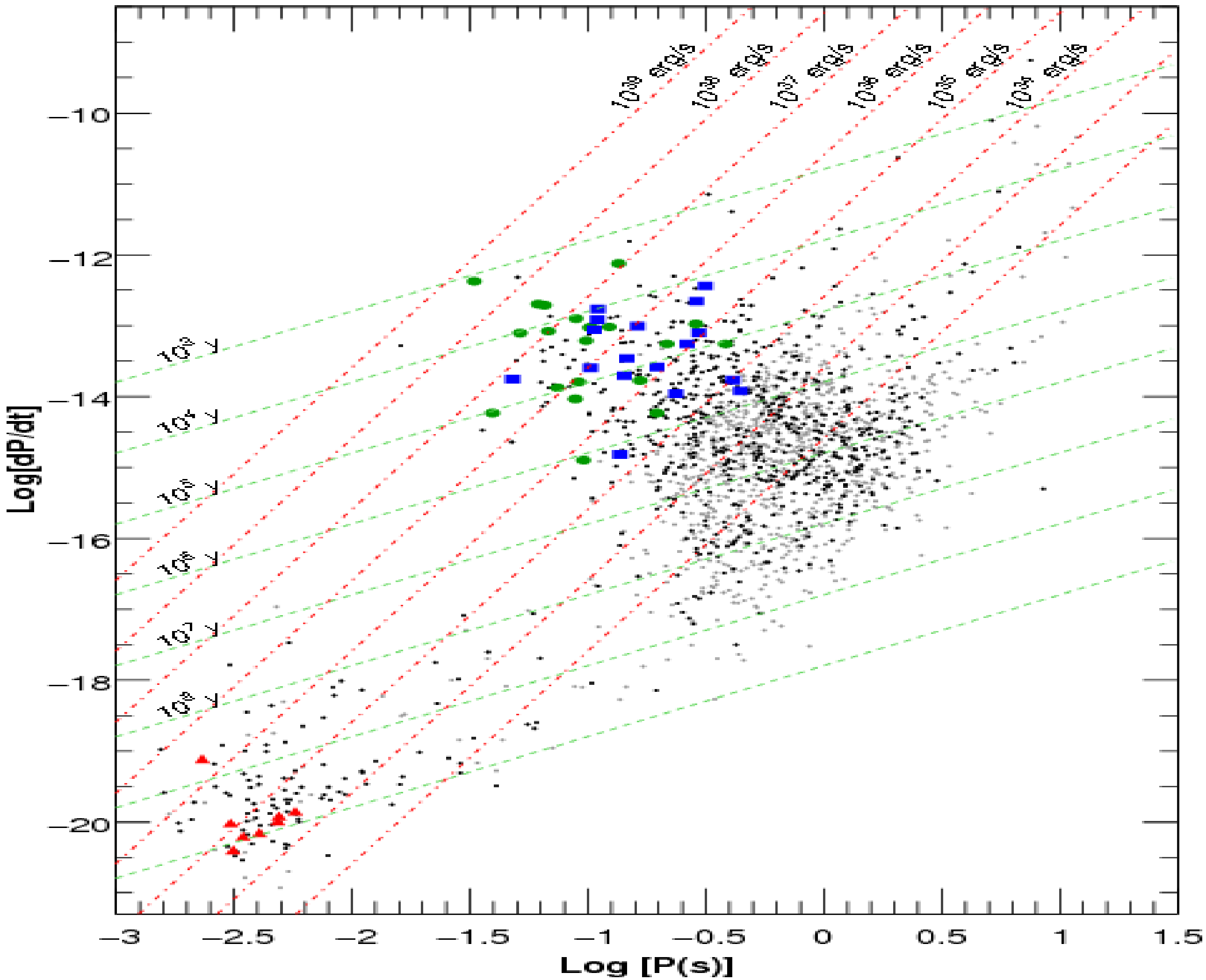

Radio and gamma-ray pulsars: what have we learned so far

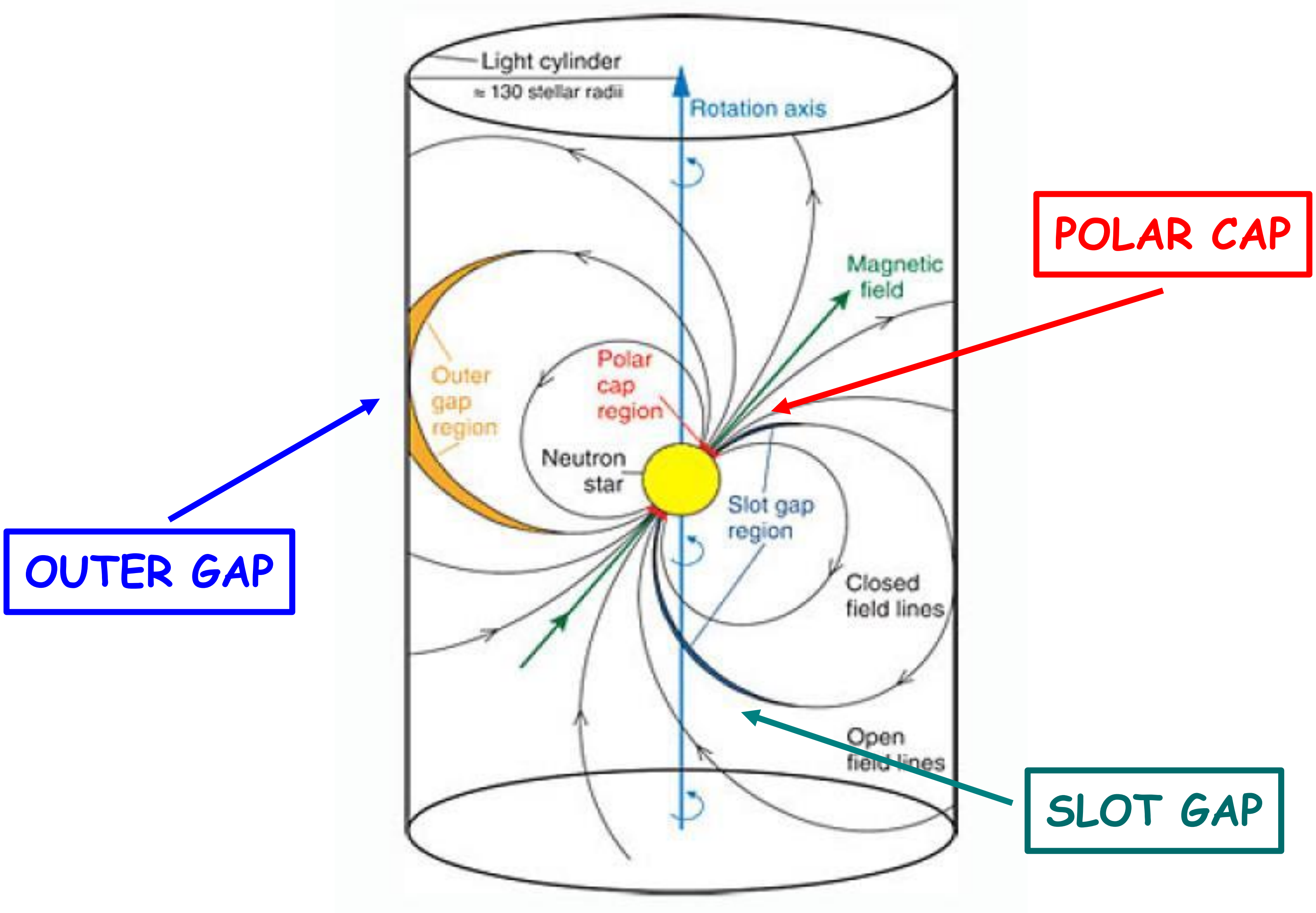

Radio and gamma-ray pulsars: what is left to do

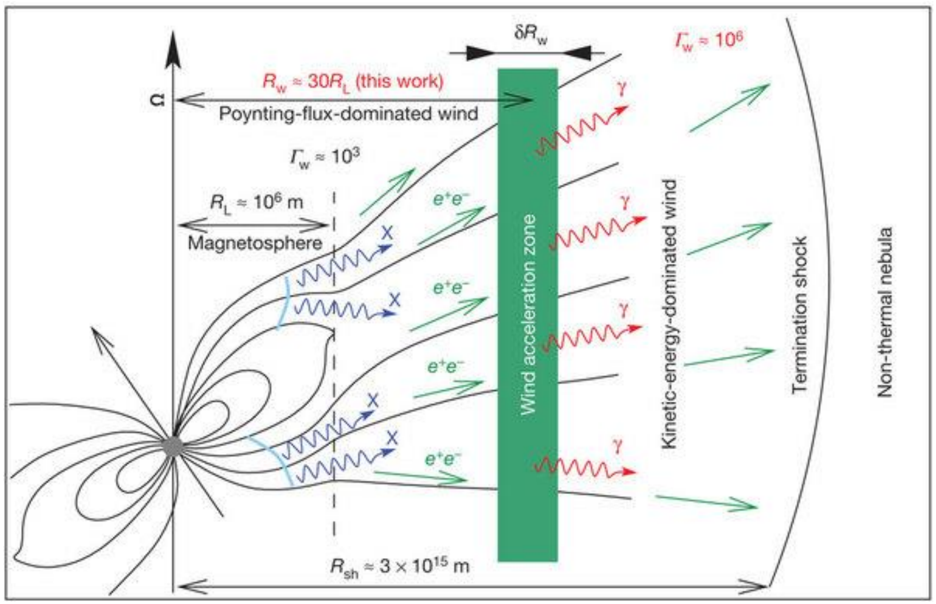

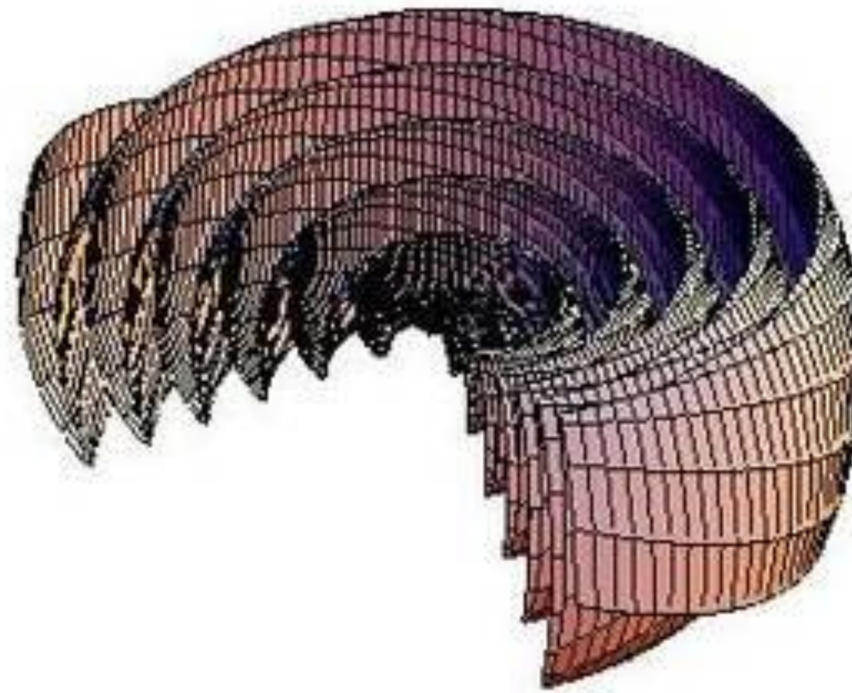

Where were we..? (2011)

AGILE detected about 20 gamma-ray pulsars

and tens of candidates from the spatial analysis

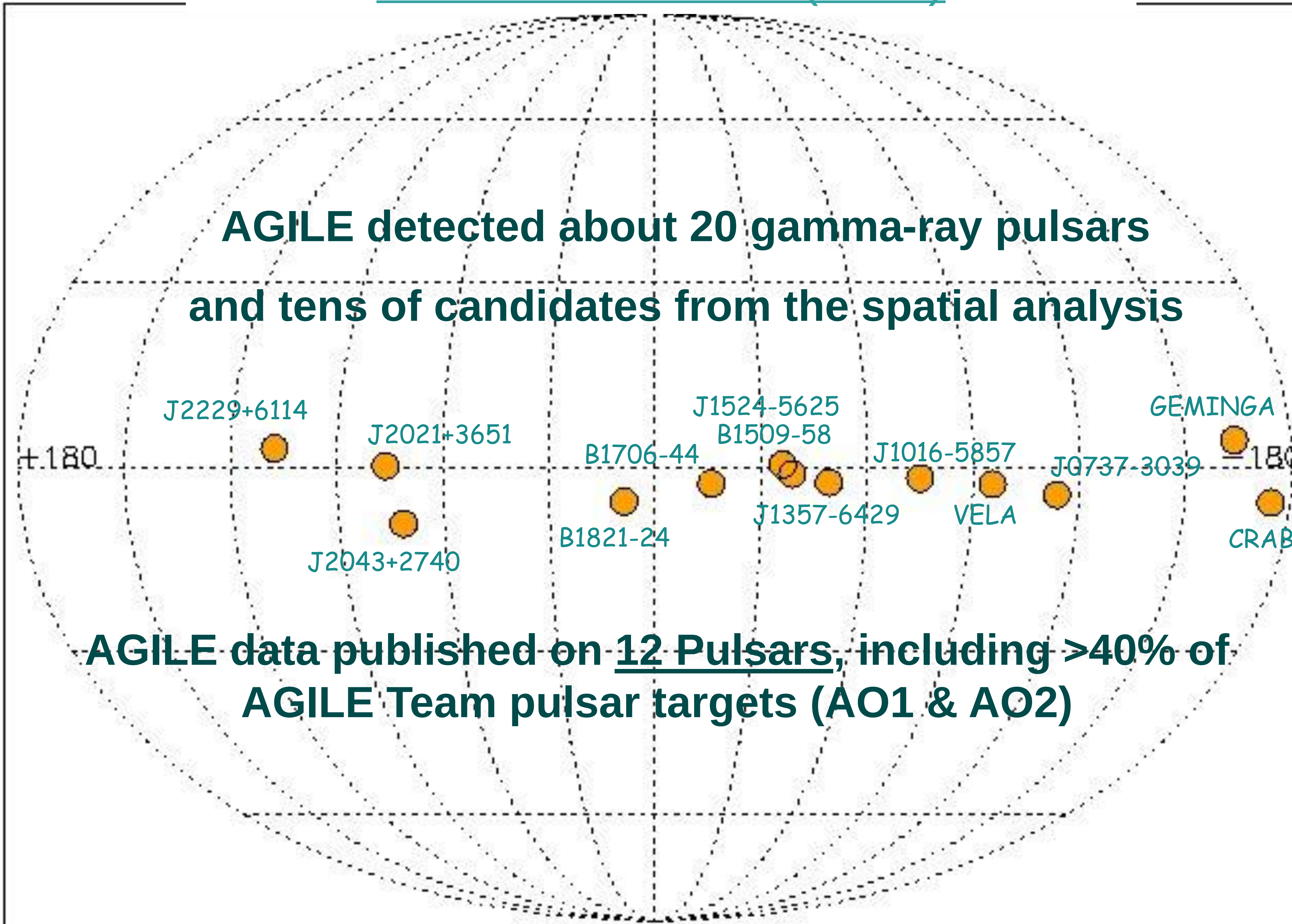

AGILE data published on <u>12 Pulsars</u>, including >40% of AGILE Team pulsar targets (AO1 & AO2)

RAS Project: Funded!

“Developement of a software tool to study pulsars from radio to gamma-rays using multi-telescope data”

P.I. Alessio Trois

Sardinia Radio Telescope

SRT
Sardinia Radio Telescope

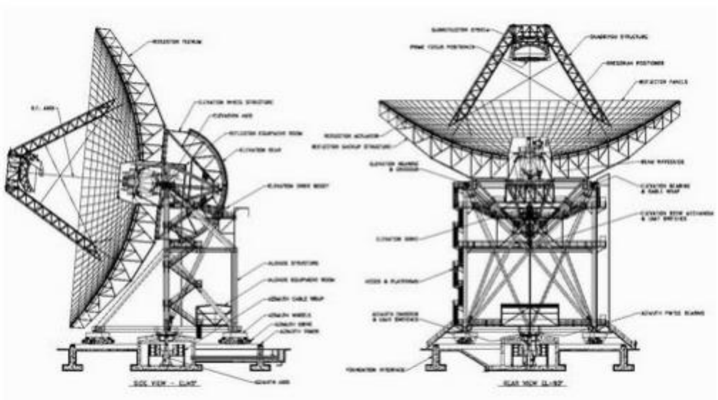

Position	Pranu Sanguni (CA), Italia
Coordinates	Lat. 39°29'50'' N - Long. 09°14'40'' E
Optics	Gregorian (shaped) + BWG
Frequency coverage	0.3÷100 GHz
Primary reflector diameter	64 m
Secondary reflector diameter	8 m
BWG reflectors diameters	2.9÷3.9 m
Multibeam receivers	22 GHz (7 feeds)
Available foci	Primary f/D = 0.33 Gregorian f/D = 2.34 2 x BWG I f/D = 1.38 2 x BWG II f/D = 2.81
Elevation range	5°÷90°
Azimut range	± 270°
Parallactic angle range	± 60°
Slew rates (wind speed < 60 km/h)	0.85 °/sec Azimuth 0.5 °/sec Elevation 10°/sec Parallactic angle
Surface accuracy (*rms* specified)	630 micron (passive surface) 185÷119 micron (active surface)
Pointing (*rms* specified)	11÷1.8 arcsec
FWHM Beamwidth	19.5 arcmin/f (GHz)
Gain	0.4÷0.7 K/Jy
First secondary lobes	≈ 20 dB under the main lobe
Receivers mounts	Primary focus : retractable positioner (4 receiver's bays) Gregorian focus : rotating turrett (8 receiver's bays) BWG I-II : fixed (4 receiver's bays)

Sardinia Radio Telescope

SRT
Sardinia Radio Telescope

Receiver	Freq.	Beam-size	T-sys [K]	Gain[%]
Primary-focus L-P band dual-frequency	305 - 410 MHz	56.2'	(65) NA	(45) NA
	1.3 - 1.8 GHz	12.6'	(21) NA	(47) NA
BWG-focus C-band mono-feed	5.7 - 7.7 GHz	2.8'	(19) 33	(66) 48
Secondary-focus K-band multi-feed	18 - 26.5 GHz	50"	(45 - 75) 70 - 90	(57) 44

The radio work described in this presentation is done with SRT commissioning data, taken during the Astronomical Validation (AV)

“Developement of a software tool to study pulsars from radio to gamma-rays using multi-telescope data”

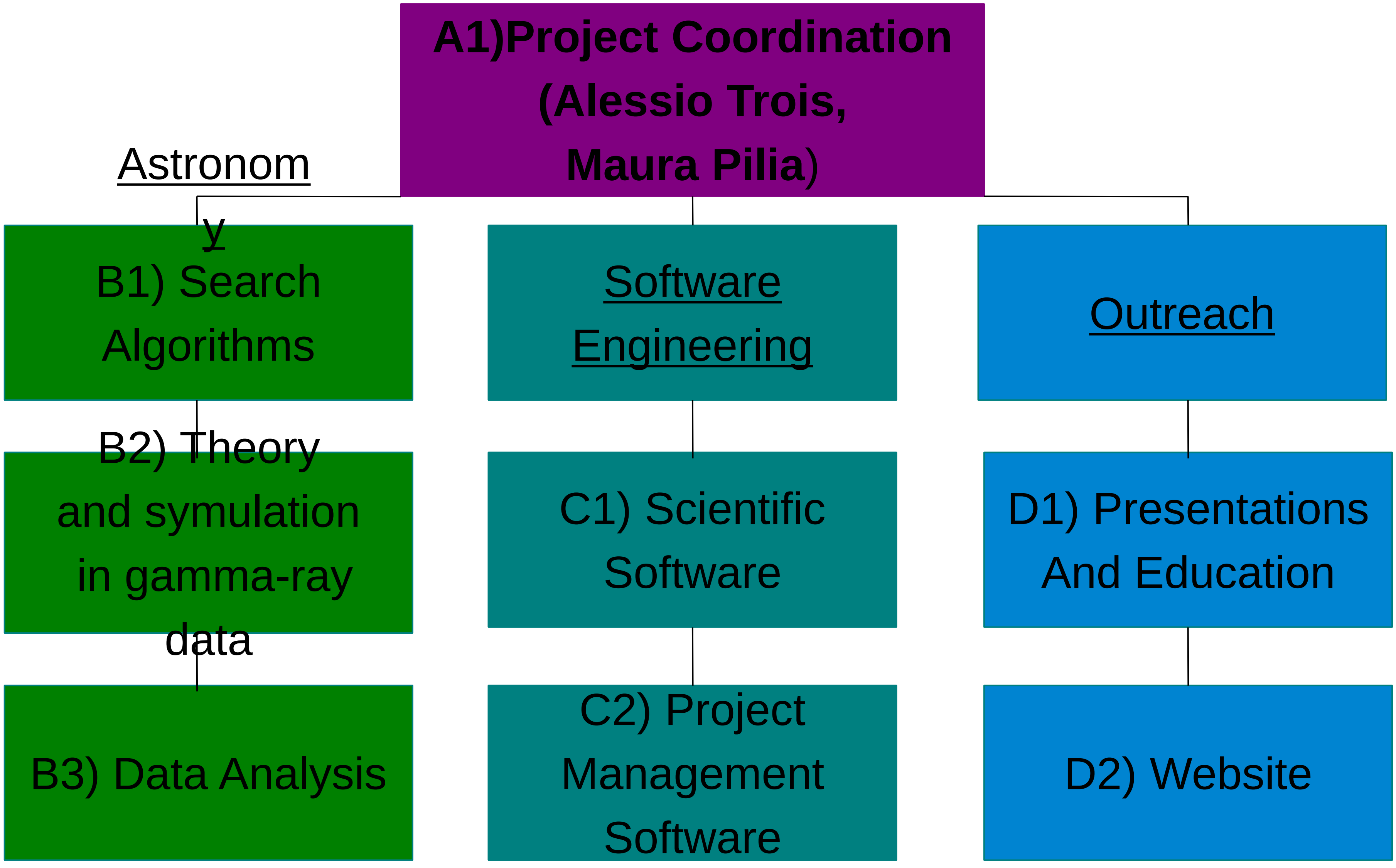

Purpose of the project is a bidirectional approach to pulsars study.

Gamma-Rays ⟷ Radio:

→ Look for counterparts of PSRs, PWNe, or UnID in radio data

← Look for new gamma-ray pulsars from SRT new discoveries and use SRT observations to time pulsars for gamma-ray observations

A multi-wavelength pulsar database

- complete
- not only gamma and radio
- automatically cross-checked
- easily accessible
- web interface
- Einstein@Home

What we have: 8 years of AGILE!

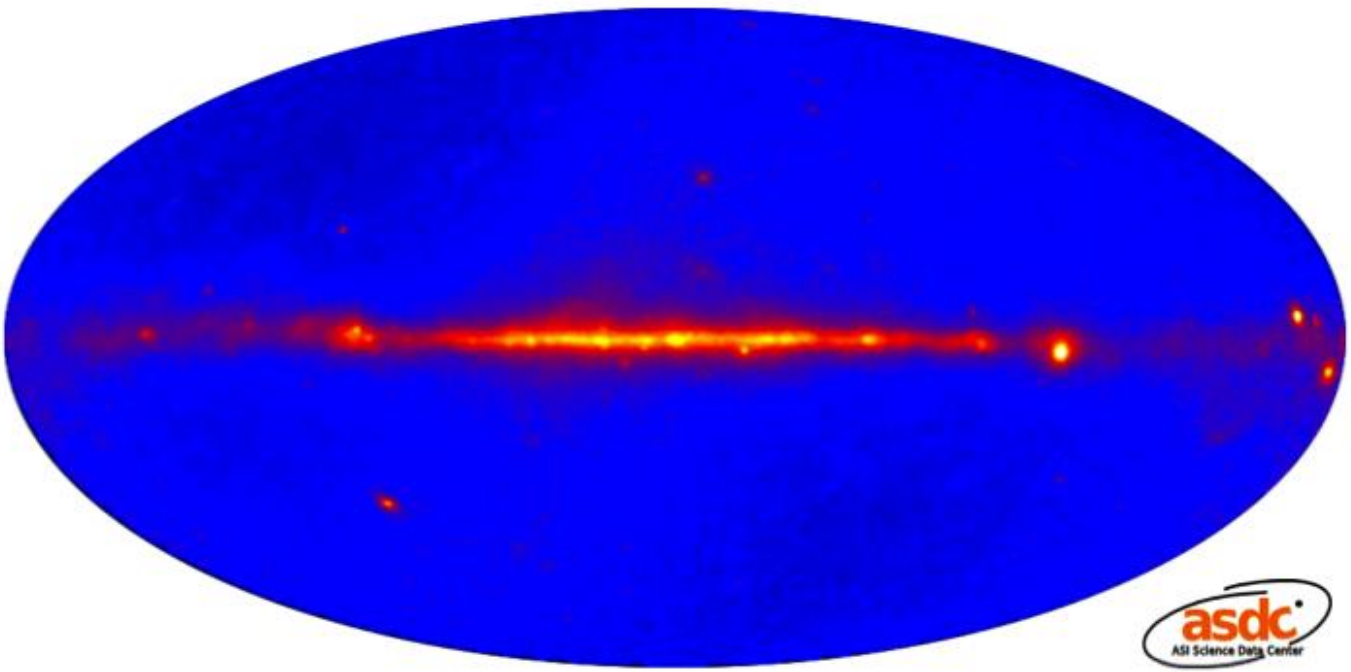

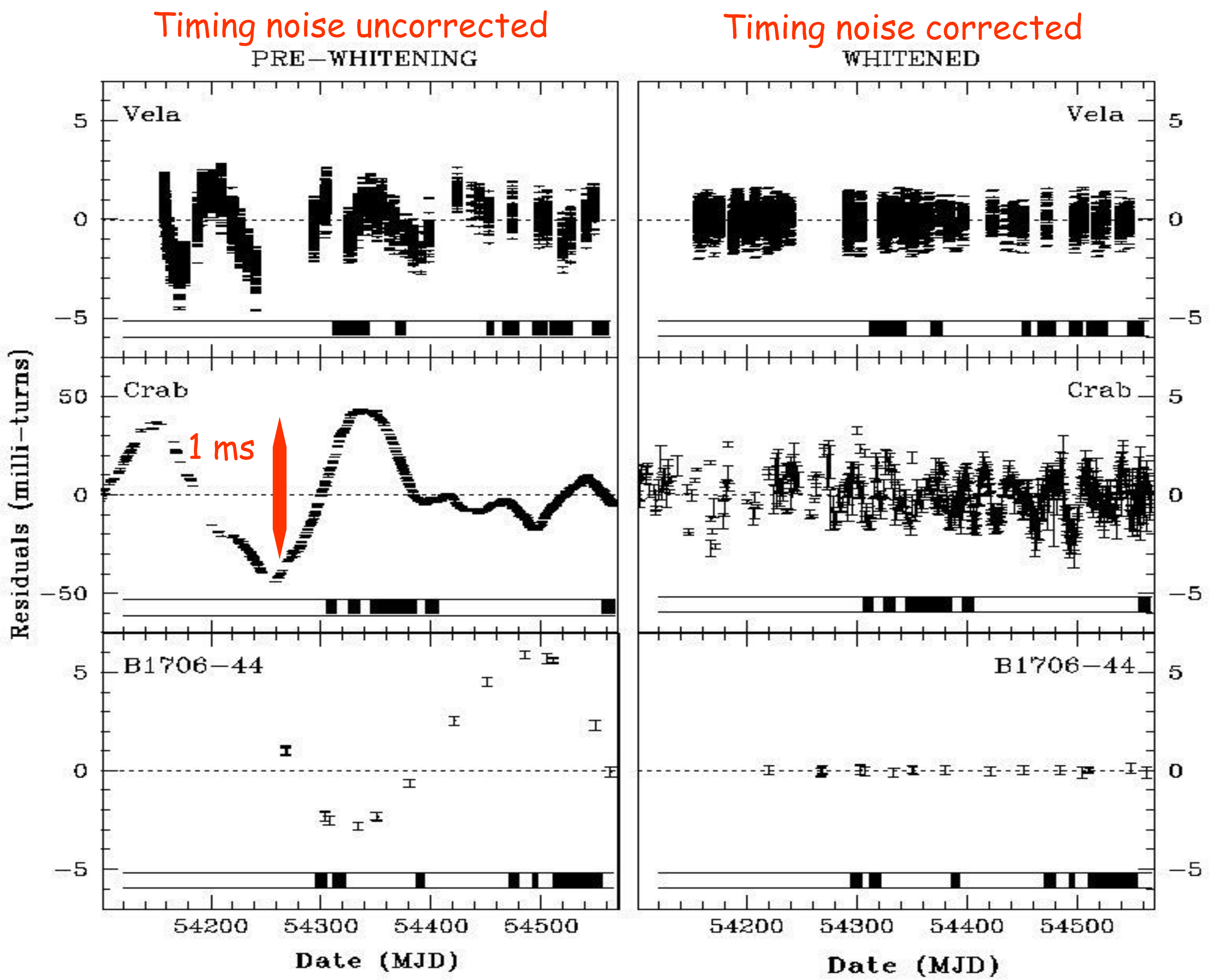

Pellizzoni et al. 2009a

Crab PSR

Gamma-ray pulsar period fit

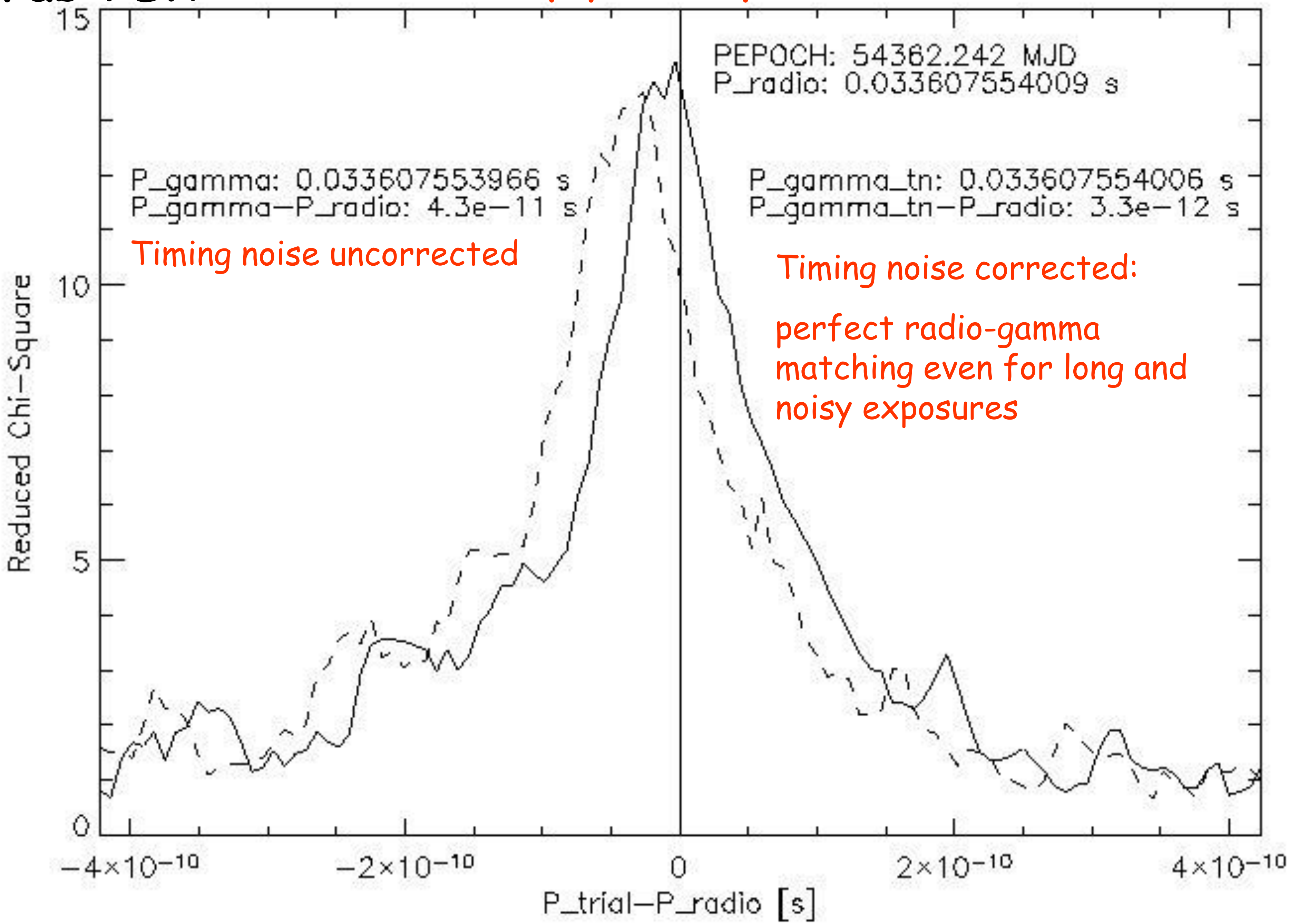

Crab PSR

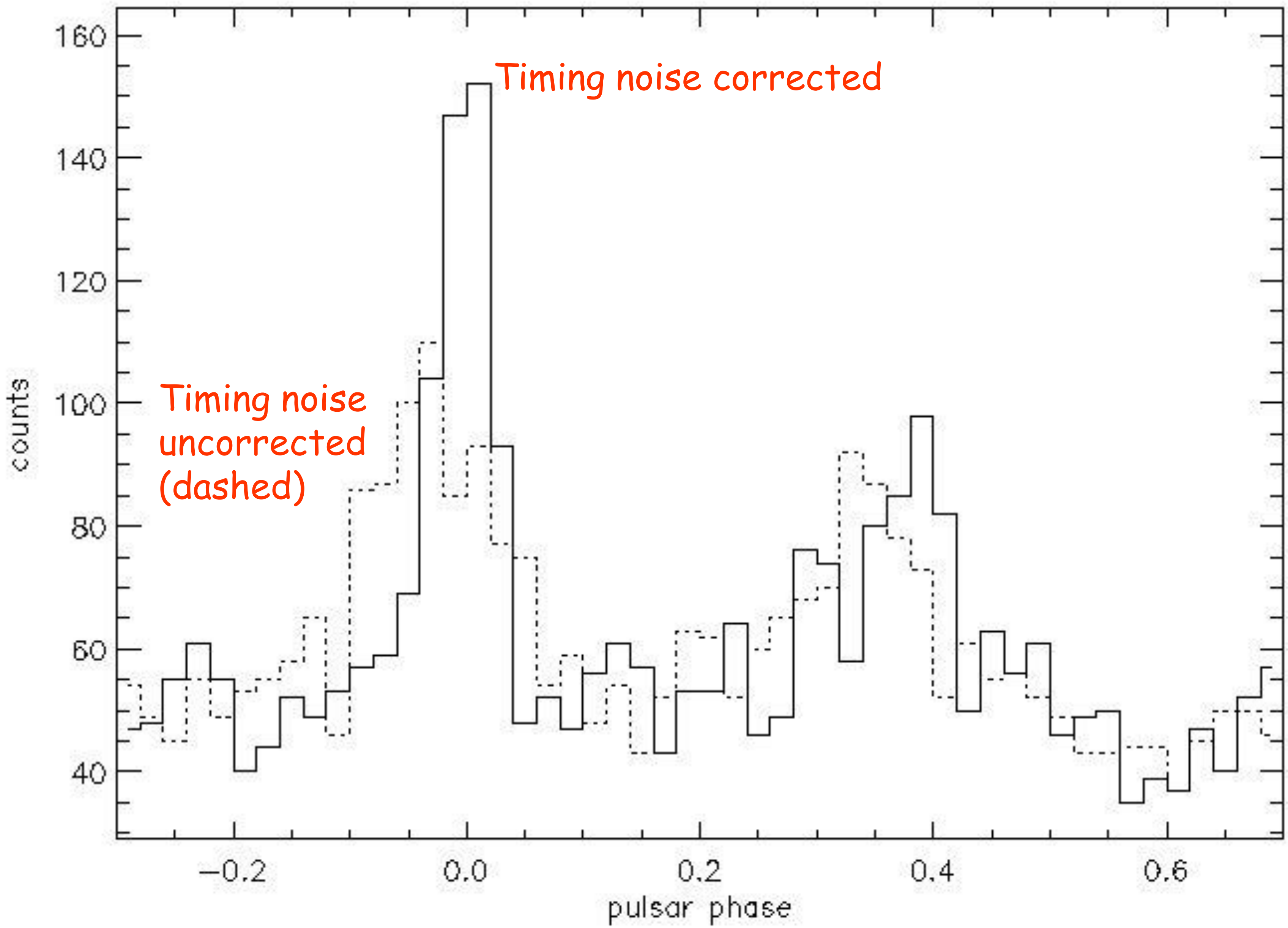

No light-curve "smearing" even in very long observations

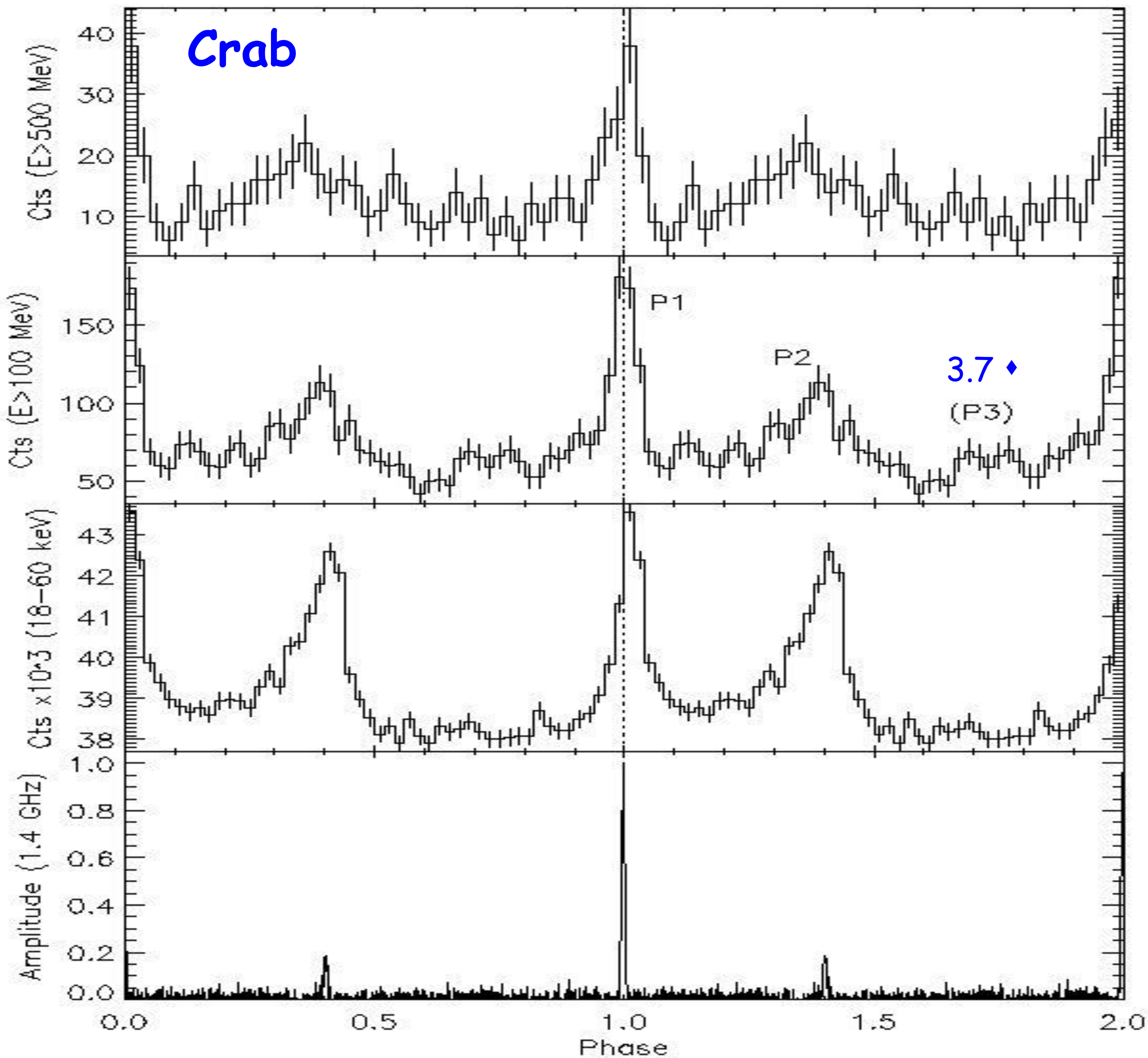

P3 is coincident with the feature HFC2 that appears in the radio profile above 4 GHz.

HFC2 polarization suggest that this peak may come from a lower emission region, near polar cap

(Moffet & Hankins; 1996, 1999)

P3: low altitude cascades?

Pellizzoni et al. 2009a

Crab pulsar with AGILE: 8 years?

Crab pulsar with AGILE: 8 years!

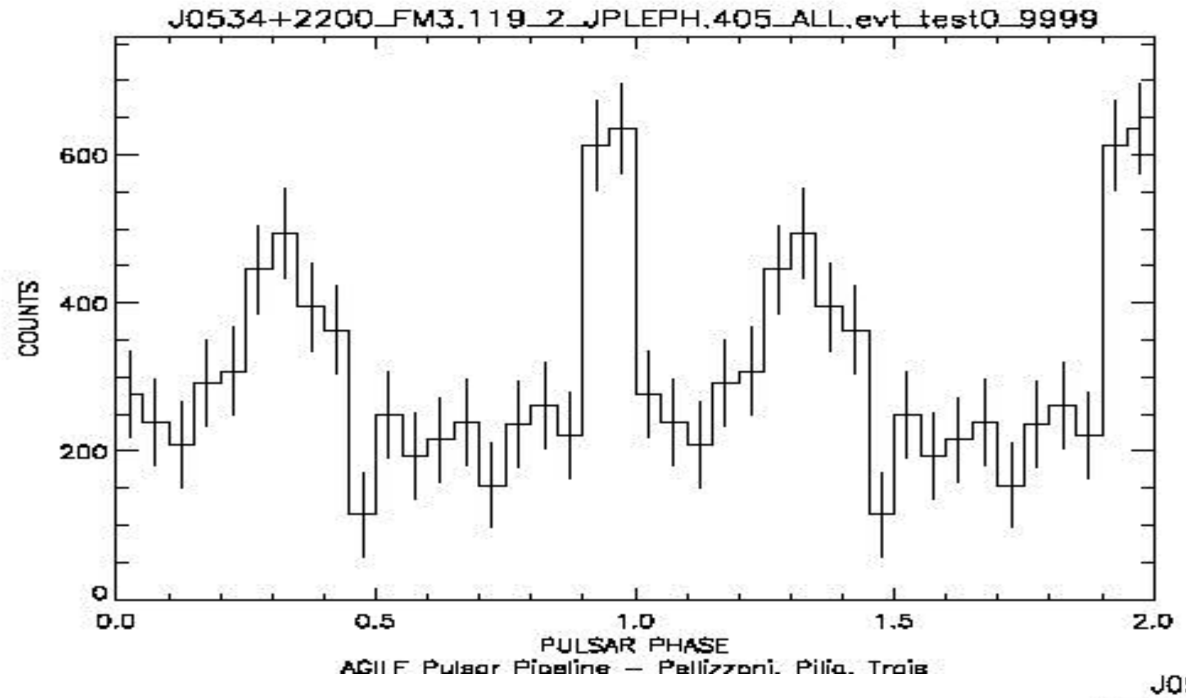

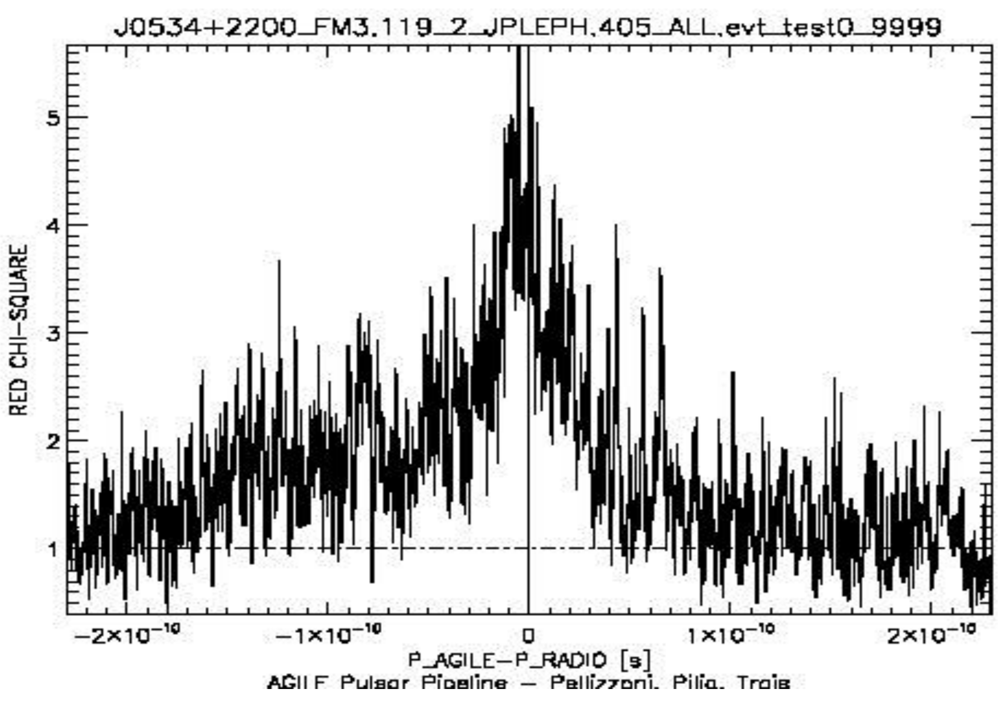

Crab pulsar with AGILE: 8 years!

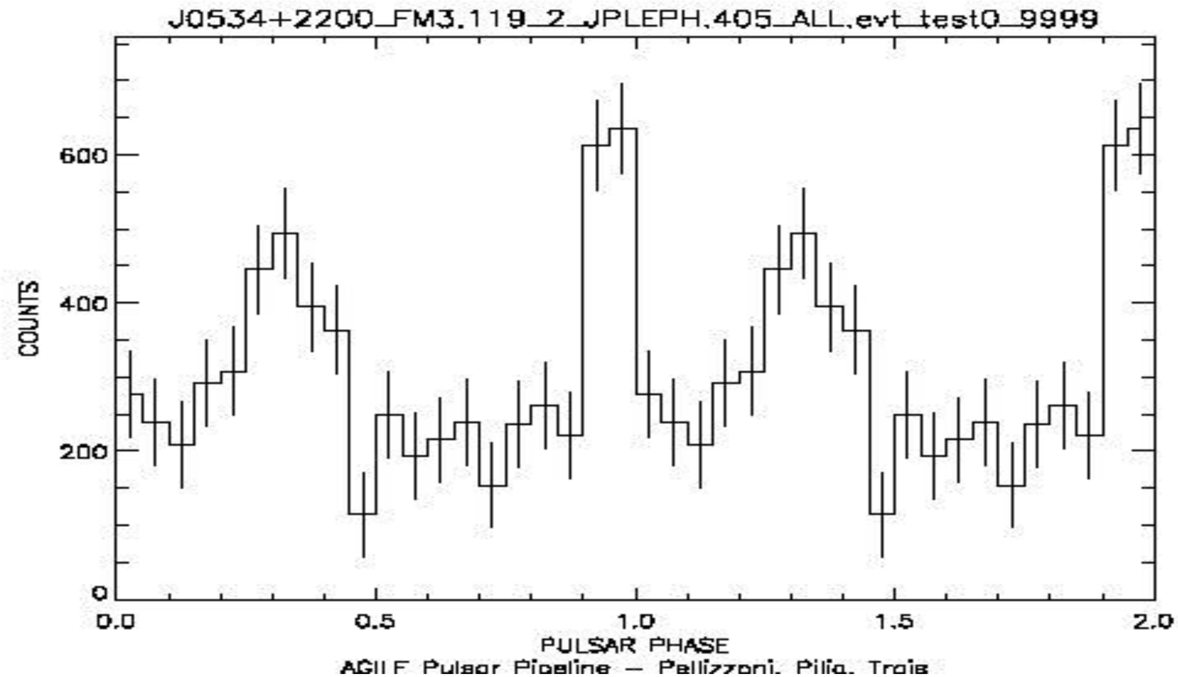

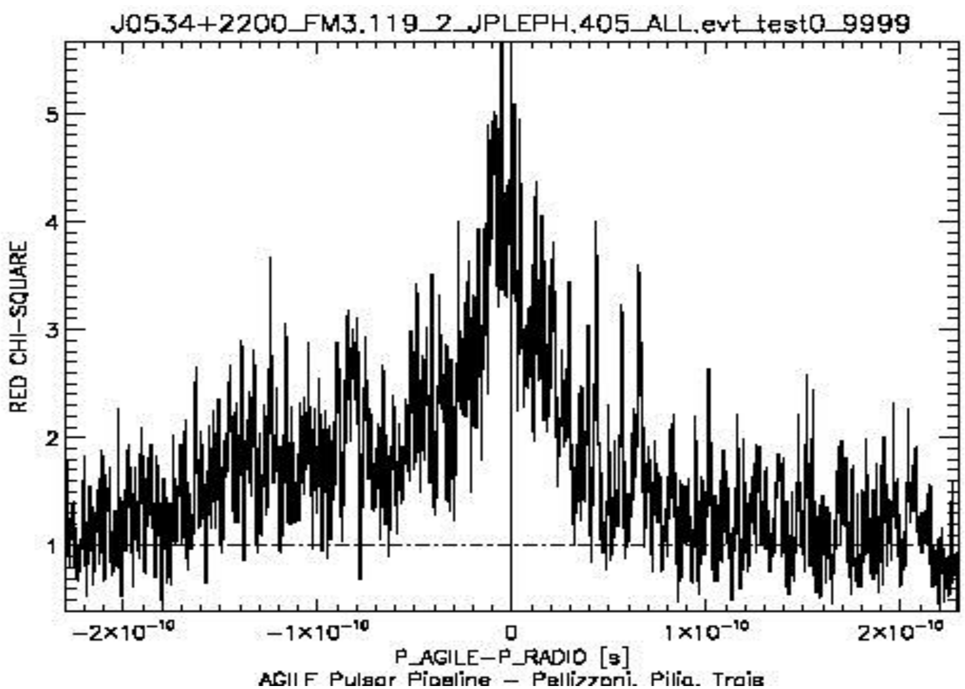

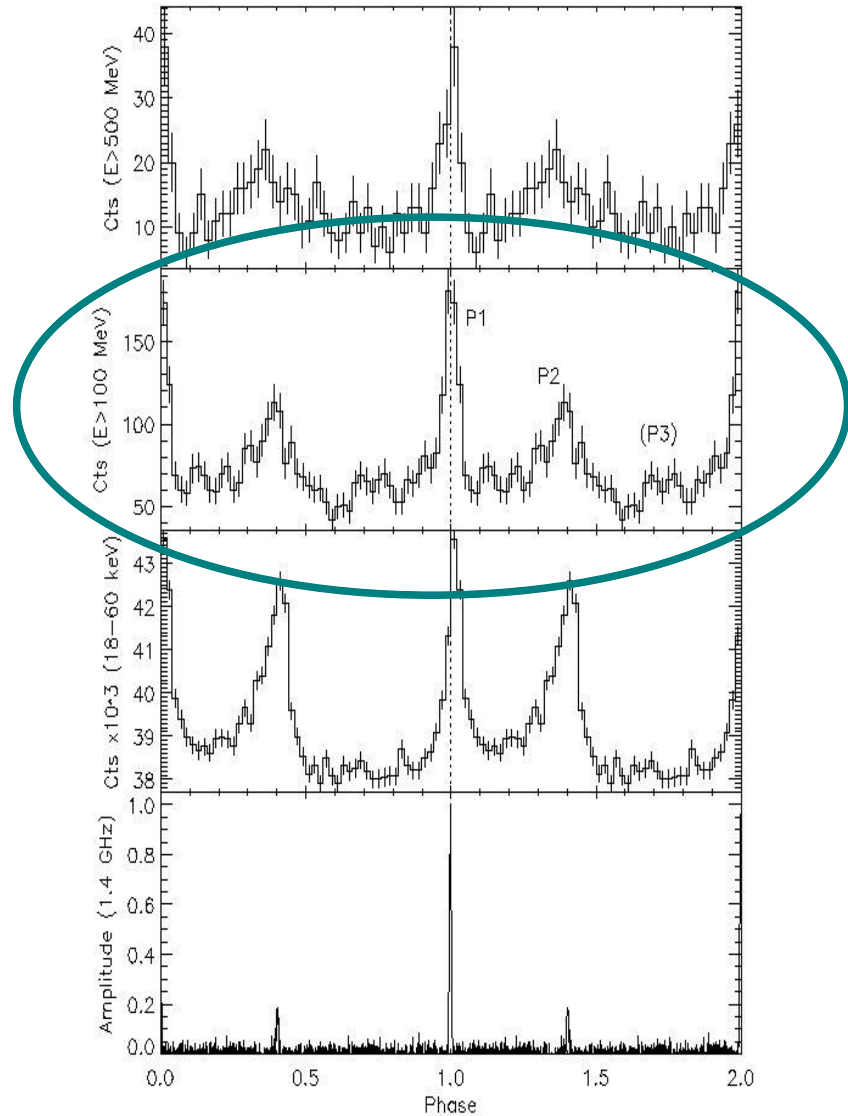

Crab pulsar with AGILE: 8 years

```
TOTAL    1.1273982e+08   3.5834314e+08       2842.6311 [DAYS]
COUNTS        81808
   1.1273982e+08   3.5834314e+08       2842.6311 [DAYS]
       1146.7357 DAYS ON TARGET
        2007           7          28       20.634899       54309.860
        2015           5          10       11.780558       57152.491
 THETA MEAN 31 THETA MIN/MAX  0 49
 ENERGY MEAN 1236 ENERGY MIN/MAX  100 49148
 DIS MEAN 3.1823255 DIS MIN/MAX  0.0045496349 4.9999379
 EVT_TYPE MEAN 0.702338
```

```
TOTAL COUNTS / ERR:                81808.0      286.021
AV. COUNTS PER BIN / ERR:          8180.80      90.4478

PULSED FRACTION:                 0.0527442
PULSED FRACTION MAX:             0.0636275
PULSED FRACTION MIN:             0.0418547

UNPULSED COUNTS / FRAC:            79650.0     0.973621
UNPULSED COUNTS / FRAC MIN:        78757.5     0.962712
UNPULSED COUNTS / FRAC MAX:        80542.5     0.984531
PULSED COUNTS / FRAC:              2158.00    0.0263788 <
PULSED COUNTS MIN / FRAC:          1265.53    0.0154695
PULSED COUNTS MAX / FRAC:          3050.47    0.0372881


FIRM PULSE DETECTION (!) <---
r.chisq=8.5617714 sigma=1.00000e+12 w.sigma=5.9262562
```

```
EPH CHECKS FINISHED.
CHECKING EPHEMERIS EPOCH RANGE...
EPHEMERIS COVERAGE:        54074.001      54566.876      492.87493 [DAYS]
AGILE DATA SPAN    :       54309.860      57152.491      2842.6311 [DAYS]
##### WARNING #####
UNVALID EPHEMERIS EPOCH RANGE: EPH_START-AG_START-EPH_FINISH-AG_FINISH
       9% COVERAGE
###################
```

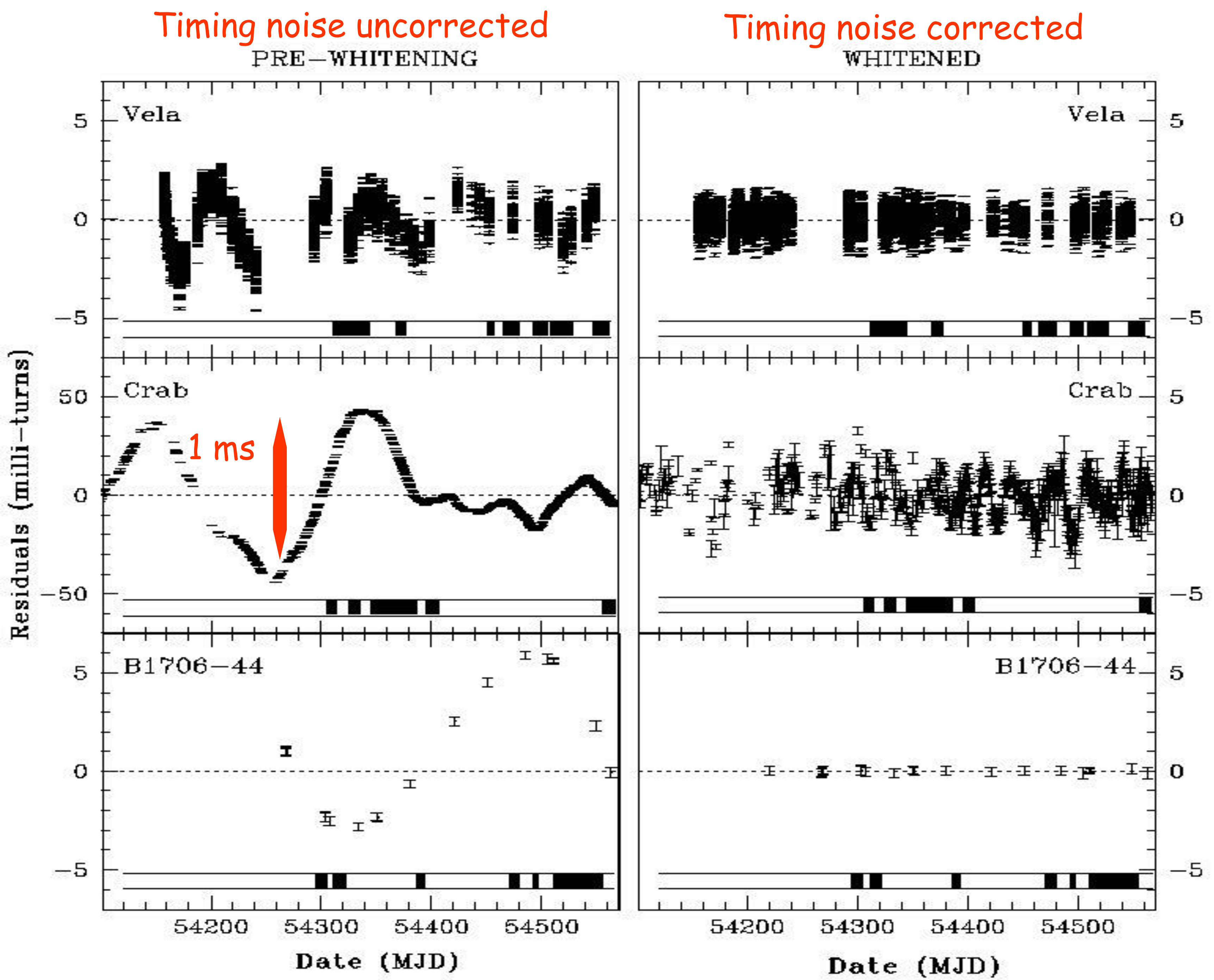

Pellizzoni et al. 2009a

How to deal with 8 years' data spans

- Addition of small data spans using JB monthly ephemeris (assuming profile stability)

How to deal with 8 years' data spans

- Addition of small data spans using JB monthly ephemeris (assuming profile stability)

- Timing with SRT

The first pulsar observations with SRT

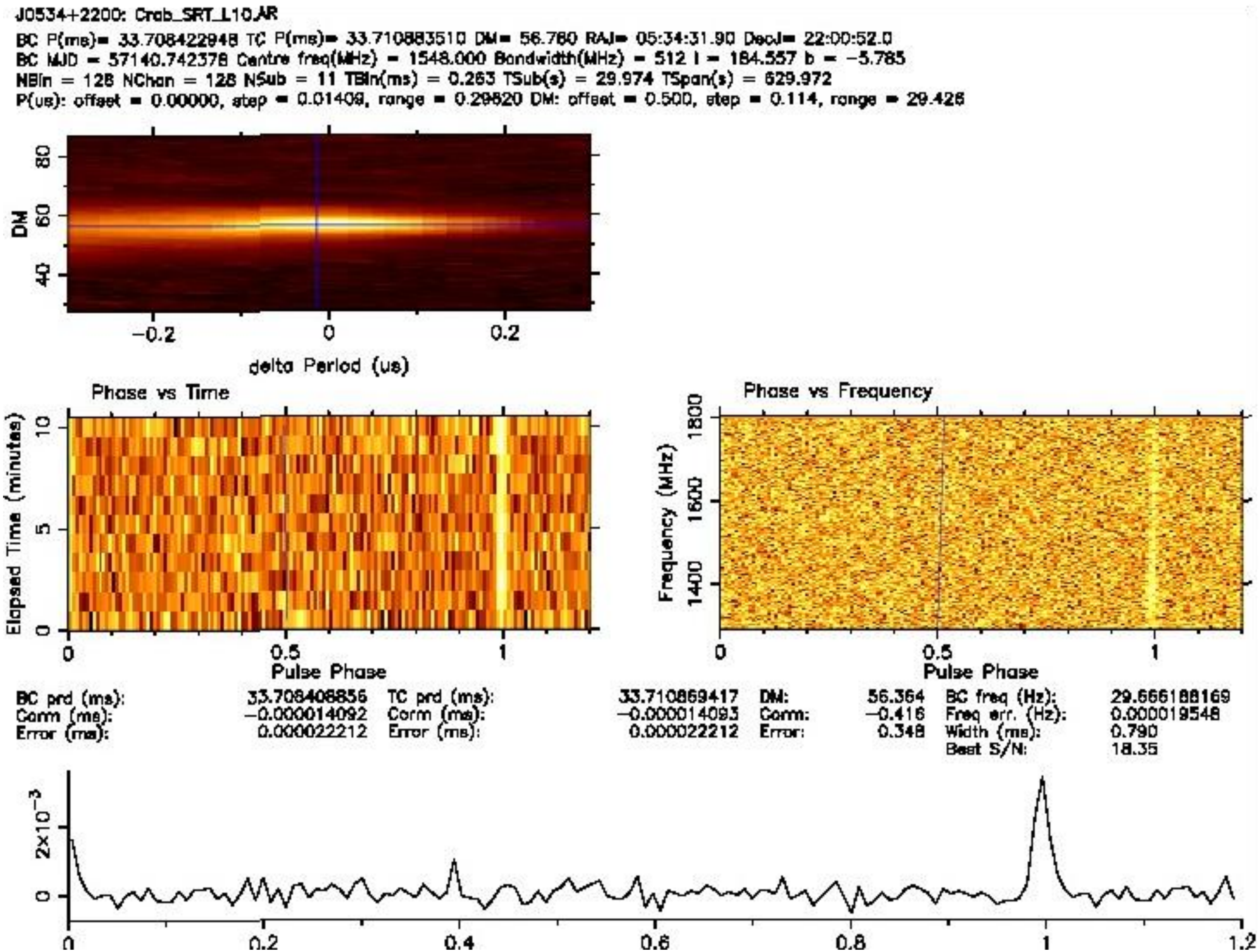

SRT Astronomical Validation Team

Hardware development


The ROACH-1 Board

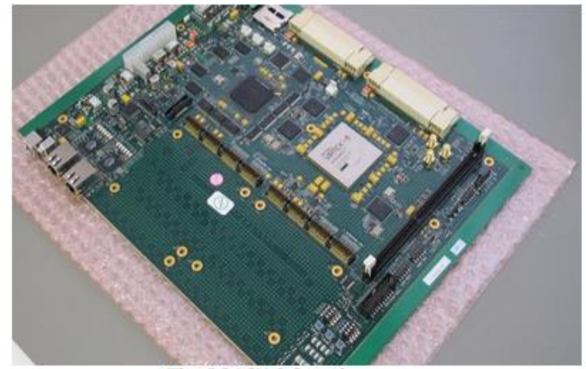
The ROACH-2 Board

ROACH 2 Boards:

-high time resolution

- high frequency resolution

-coherent dedispersion

ROACH
Reconfigurable Open Architecture Computing Hardware

Melis, Concu, Trois

How to deal with 8 years' data spans

- Addition of small data spans using JB monthly ephemeris (assumes profile stability)
- Timing with SRT

- Timing in gamma-rays?

From SRT to Fermi to.. AGILE?

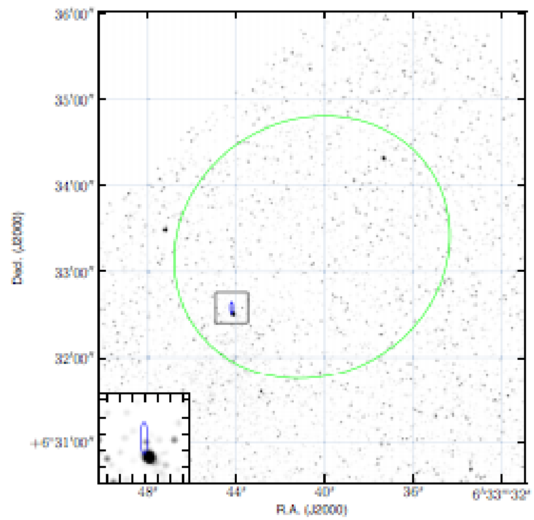

Figure 10. Timing position for PSR J0633+0632 (blue ellipse). The large ellipse is the LAT position of 1FGL J0633.7+0632, based on 18 months of data. The background 0.5–8 keV X-ray image is a 20 ks *Chandra* ACIS-S image (ObsID 11123), smoothed with a Gaussian with $\sigma = 0''.5$. The inset shows a 10'' region around the timing location.

(A color version of this figure is available in the online journal.)

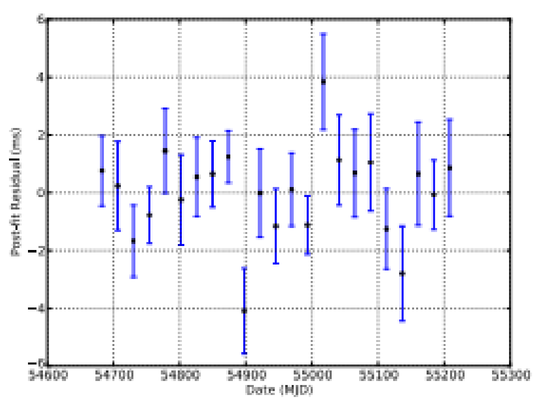

Figure 11. Post-fit timing residuals for PSR J0633+0632.

(A color version of this figure is available in the online journal.)

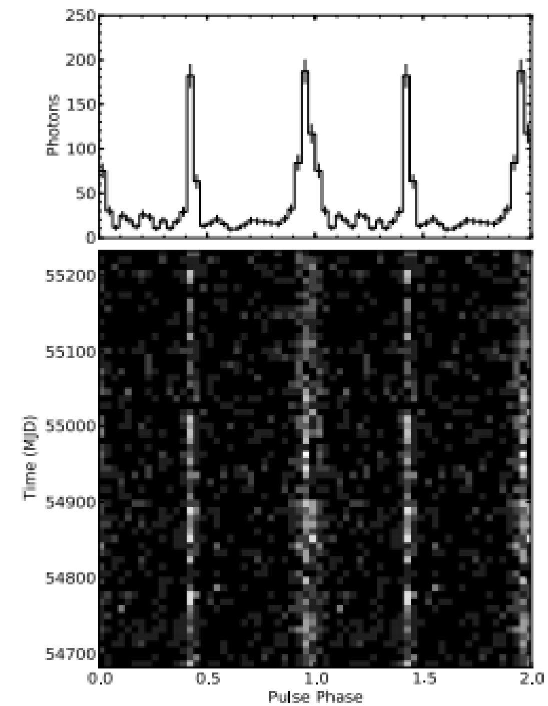

Figure 12. Two-dimensional phaseogram and pulse profile of PSR J0633+0632. Two rotations are shown on the *X*-axis. The photons were selected according to the ROI and E_{min} in Table 4. The fiducial point corresponding to TZRMJD is phase 0.0.

Table 4
PSR J0633+0632

Parameter	Value
R.A., α (J2000.0)	06:33:44.21 $\pm 0^s.02$
Decl., δ (J2000.0)	+06:32:34.9 $\pm 1''.6$
Monte Carlo position uncertainty	$3''.5$
Pulse frequency, ν (s^{-1})	3.3625291588(7)
Frequency first derivative, $\dot{\nu}$ (s^{-2})	$-8.9991(3) \times 10^{-13}$
Frequency second derivative, $\ddot{\nu}$ (s^{-3})	$-2(1) \times 10^{-23}$
Epoch of frequency (MJD)	54945
TZRMJD	54945.385967311181439
Number of photons (n_γ)	1174
Number of TOAs	23
rms timing residual (ms)	1.4
Template profile	2 Gaussian
E_{min}	550 MeV
ROI	$0^\circ.6$
Valid range (MJD)	54682–55208

Ray et al. 2011

AGILE

Fermi

20 MeV – 50 GeV

20 MeV – **300 GeV**

In the 30-100 MeV AGILE sensitivity is competitive (500 cm^2 eff. Area for timing).

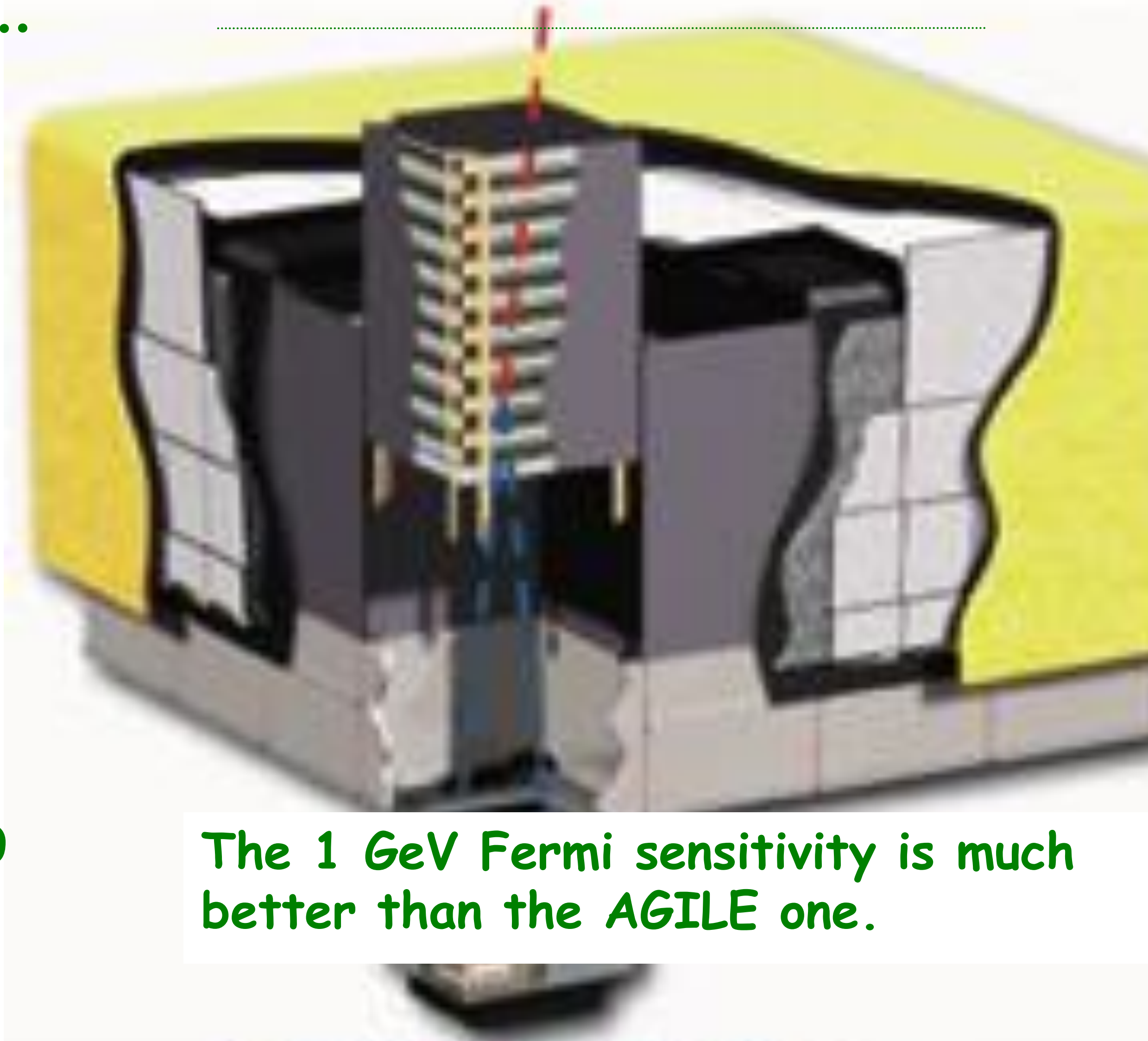

The 1 GeV Fermi sensitivity is much better than the AGILE one.

PSR B1509-58 with AGILE

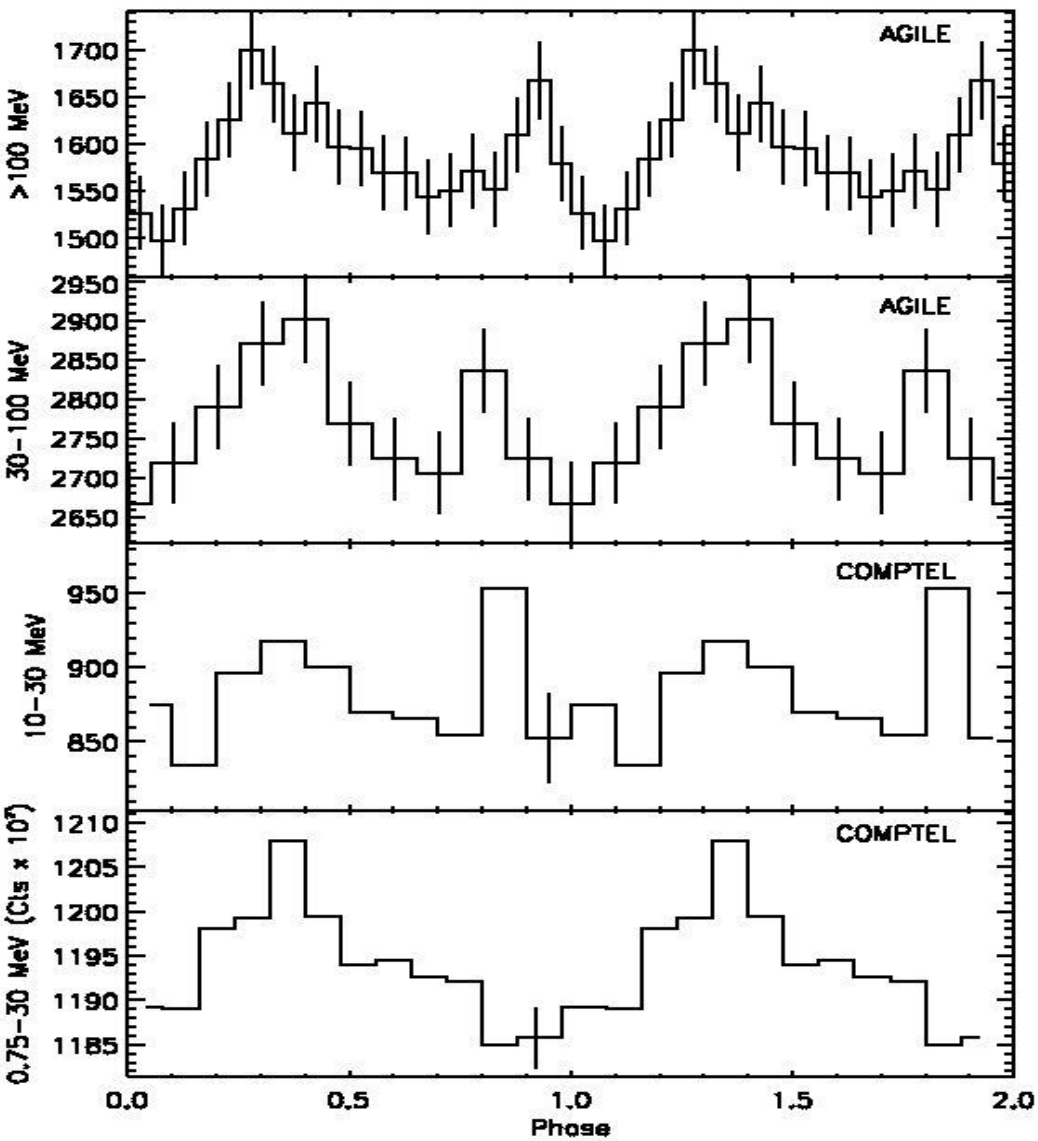

Pellizzoni et al. ApJ, 695, L115, 2009

Pilia et al. ApJ, 723, 707, 2010

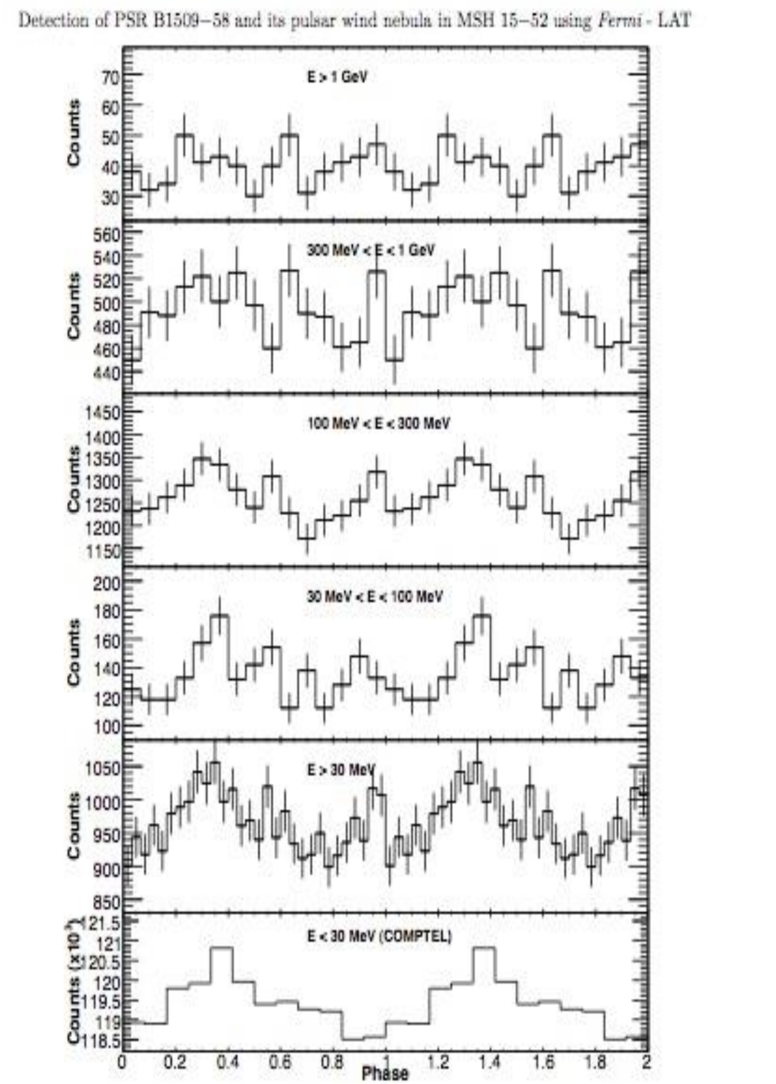

FIG. 2.— Light curves of the pulsar PSR B1509−58 in different energy bands within a circular region of energy-dependent radius. From bottom to the top: COMPTEL (0.75 – 30 MeV; Kuiper et al 1999) and LAT profiles in 30 MeV–300 GeV, 30 MeV–100 MeV, 100 MeV–300 MeV, 300 MeV–1 GeV, 1 GeV–300 GeV energy bands are presented. Two cycles are shown.

Abdo et al. ApJ, 714, 927, 2010

Interpretation

Our observations are compatible with emission from the polar cap regions powered by photon splitting cascades.

This likely inerpretation could represent the first physical measurement ever made related to the QED photon splitting process.

The fact that PC emission at HE appears rare might be explained by the requirement that a number of conditions concur to have low magnetospere emission, e.g. an aligned geometry and high magnetic fields.

New class of "soft" gamma-ray pulsars?

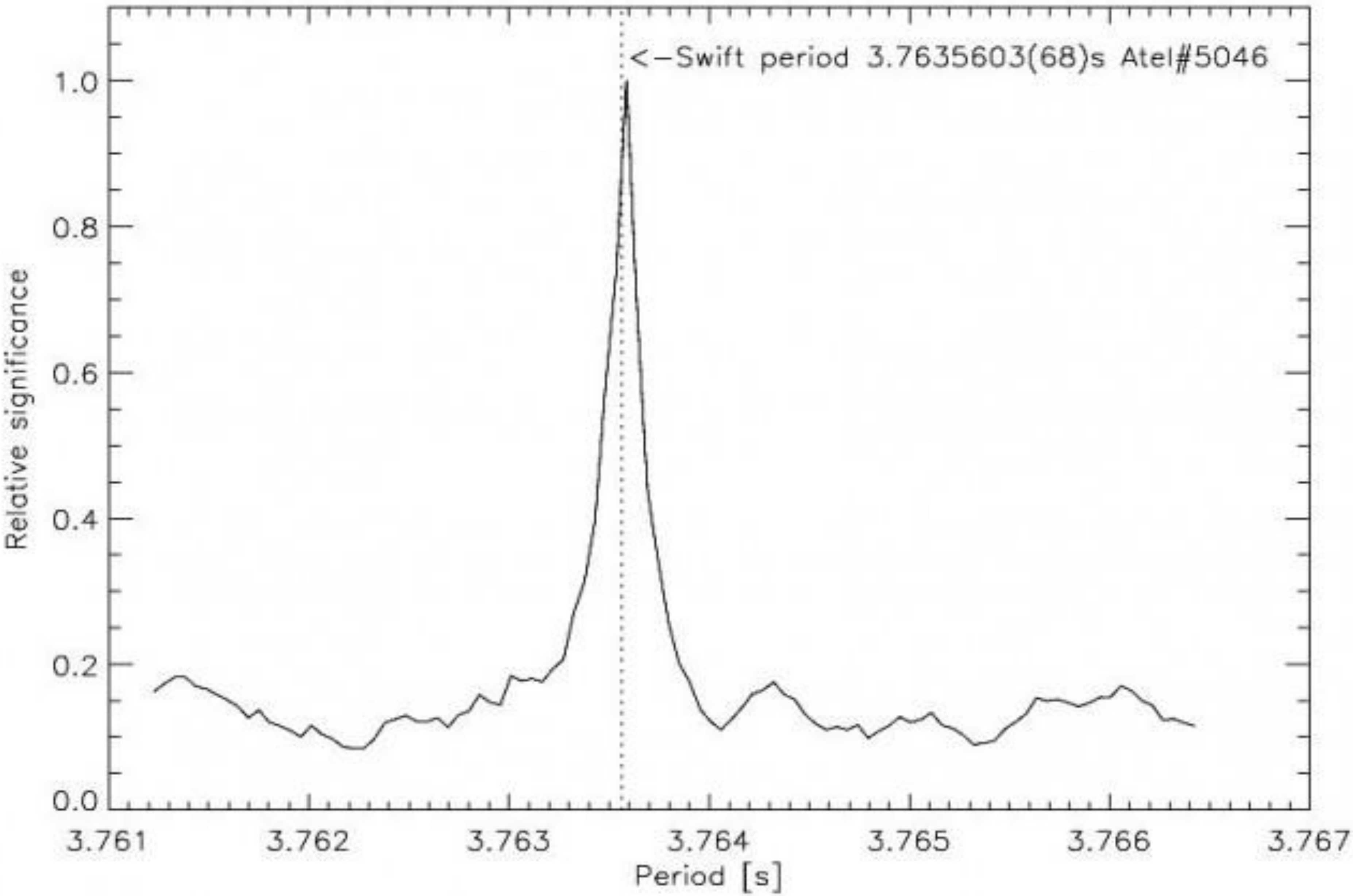

Detection of the magnetar PSR J1745-2900 with SRT
(7.3 GHz, 730 MHz, 40 ms int.): ATEL#5053
(Cagliari Pulsar and Multi-wavelength Group)

First tests

Table 9: *Values, for each pointing, of the minimum detectable radio flux* S_{min} *(with* $\Delta t = 3600$ s*), and the integration time* Δt *(with* $S_{1400,min} = 0.15$ *mJy) at SRT according to the pulsar type and its position with respect to the Galactic plane.*
We recall that S scales as $S \propto \nu^{\alpha}$ *(with* $\alpha = -1.7$*), therefore at SRT* $S_{1400,min} = 0.15$ *mJy becomes* $S_{P,min} = 1.527$ *mJy,* $S_{L,min} = 0.126$ *mJy,* $S_{C,min} = 0.011$ *mJy,* $S_{K,min} = 0.001$ *mJy.*

Type	Band	Plane		Out		Centre	
		S_{min} [mJy]	Δt [s]	S_{min} [mJy]	Δt [s]	S_{min} [mJy]	Δt [s]
Ordinary	P	0.51846	$4.14820 \cdot 10^{2}$	0.37294	$2.14630 \cdot 10^{2}$	1.21186	$2.26636 \cdot 10^{3}$
	L	0.04651	$4.89309 \cdot 10^{2}$	0.04541	$4.66271 \cdot 10^{2}$	0.05229	$6.18334 \cdot 10^{2}$
	C	0.03107	$3.16699 \cdot 10^{4}$	0.03106	$3.16508 \cdot 10^{4}$	0.03112	$3.17692 \cdot 10^{4}$
	K	0.08268	$1.32724 \cdot 10^{7}$	0.08267	$1.32723 \cdot 10^{7}$	0.08268	$1.32731 \cdot 10^{7}$
Millisecond	P	2.93314	$1.32767 \cdot 10^{4}$	2.05458	$6.51430 \cdot 10^{3}$	8.45917	$1.10428 \cdot 10^{5}$
	L	0.09236	$1.92916 \cdot 10^{3}$	0.09016	$1.83833 \cdot 10^{3}$	0.10382	$2.43786 \cdot 10^{3}$
	C	0.06124	$1.23034 \cdot 10^{5}$	0.06122	$1.22960 \cdot 10^{5}$	0.06133	$1.23421 \cdot 10^{5}$
	K	0.16295	$5.15591 \cdot 10^{7}$	0.16295	$5.15586 \cdot 10^{7}$	0.16295	$5.15617 \cdot 10^{7}$

Note – Column 1 and 2 list the pulsar type the observing band; columns 3 and 4 list S_{min} and Δt for pulsars in the Galactic plane; columns 5 and 6 list S_{min} and Δt for pulsars outside the Galactic plane; columns 7 and 8 list S_{min} and Δt for pulsars near the center of the Galactic plane.

Credit Marco Marongiu

First candidates, continuously updating

Table 7: *Sample of 22 gamma-ray sources potentially observable by SRT for the search of new radio and/or gamma-ray pulsars, sorted by energy flux* G_{100}.

Gamma-ray source	ra [deg]	dec [deg]	s_{max} [deg]	s_{min} [deg]	l [deg]	b [deg]	G_{100} [(a)]	$n_{punt\,P}$	$\Delta n_{punt\,P}$	$n_{punt\,L}$	$\Delta n_{punt\,L}$	$n_{punt\,C}$	$\Delta n_{punt\,C}$
3FGL J1848.4-0141	282.11	-1.69	0.080	0.057	31.088	-0.11	1.14	0.022	0.030	0.41	0.565	7.84	10.55
3FGL J1839.3-0552	279.84	-5.88	0.034	0.028	26.327	-0.01	1.00	0.004	0.013	0.08	0.251	1.63	4.698
3FGL J1906.6+0720	286.67	7.333	0.037	0.027	41.192	-0.02	0.99	0.004	0.013	0.09	0.260	1.69	4.863
3FGL J1852.8+0158	283.20	1.972	0.062	0.055	34.847	0.587	0.82	0.016	0.025	0.31	0.477	5.91	8.927
3FGL J1857.9+0210	284.49	2.170	0.060	0.057	35.607	-0.46	0.68	0.016	0.025	0.31	0.474	5.87	8.867
3FGL J2017.9+3627	304.48	36.45	0.034	0.031	74.541	0.410	0.65	0.005	0.014	0.09	0.266	1.85	4.975
3FGL J1850.5-0024	282.63	-0.40	0.054	0.043	32.468	0.017	0.57	0.011	0.021	0.21	0.397	4.03	7.432
3FGL J1857.2+0059	284.31	0.986	0.042	0.035	34.471	-0.84	0.48	0.007	0.016	0.13	0.315	2.56	5.889
3FGL J1919.9+1407	289.98	14.11	0.077	0.061	48.710	0.241	0.46	0.023	0.030	0.43	0.566	8.14	10.58
3FGL J2004.4+3338	301.10	33.64	0.035	0.033	70.671	1.185	0.43	0.005	0.014	0.10	0.275	1.98	5.138
3FGL J0223.6+6204	35.906	62.08	0.039	0.035	133.49	1.115	0.39	0.006	0.015	0.12	0.300	2.36	5.617
3FGL J2038.4+4212	309.62	42.20	0.058	0.053	81.527	0.542	0.39	0.015	0.024	0.28	0.453	5.34	8.472
3FGL J1857.9+0355	284.48	3.927	0.071	0.063	37.170	0.342	0.37	0.022	0.029	0.41	0.548	7.78	10.25
3FGL J1901.5-0126	285.39	-1.44	0.055	0.053	32.801	-2.92	0.36	0.014	0.023	0.27	0.439	5.04	8.215
3FGL J1849.5-0124c	282.39	-1.41	0.076	0.066	31.463	-0.23	0.34	0.024	0.030	0.46	0.578	8.60	10.80
3FGL J1653.6-0158	253.41	-1.98	0.035	0.034	16.618	24.92	0.33	0.005	0.014	0.11	0.281	2.07	5.251
3FGL J2041.1+4736	310.28	47.60	0.050	0.048	86.091	3.461	0.31	0.011	0.021	0.22	0.399	4.16	7.455
3FGL J1827.6-0846	276.90	-8.77	0.053	0.047	22.418	1.241	0.30	0.012	0.021	0.23	0.408	4.32	7.627
3FGL J1838.9-0646	279.72	-6.77	0.078	0.059	25.477	-0.31	0.29	0.022	0.029	0.41	0.558	7.80	10.43
3FGL J1844.3-0344	281.10	-3.74	0.056	0.046	28.795	-0.14	0.28	0.012	0.022	0.23	0.416	4.45	7.786
3FGL J1837.6-0717	279.40	-7.29	0.086	0.057	24.866	-0.26	0.26	0.023	0.031	0.44	0.591	8.40	11.05
3FGL J2034.4+3833c	308.62	38.56	0.052	0.051	78.158	-1.04	0.26	0.013	0.022	0.24	0.421	4.65	7.879

[a] In units of 10^{-10} erg s^{-1} cm^{-2}.
[b] The number of σ of detection is approximately associated with the square root of $signif_{avg}$.

Note — Column 1 lists the name of gamma-ray source; columns 2 and 3 list the right ascension and the declination of the gamma-ray source (ra and dec); columns 4 and 5 list the semi-major and the semi-minor axis of the error box (elliptical in shape) at 95% confidence (s_{max} and s_{min}); columns 6 and 7 list the galactic longitude and the galactic latitude (l and b); column 8 lists the energy flux in range 0.1 – 100 GeV (G_{100}); columns 9 and 10 list the number of pointings practicable by SRT in P-band ($\nu_0 = 0.3575$ GHz) and its uncertainties ($n_{punt\,P}$, $\Delta n_{punt\,P}$); columns 11 and 12 list the number of pointings practicable by SRT in L-band ($\nu_0 = 1.55$ GHz) and its uncertainties ($n_{punt\,L}$, $\Delta n_{punt\,L}$); columns 13 and 14 list the number of pointings practicable by SRT in C-band ($\nu_0 = 6.7$ GHz) and its uncertainties ($n_{punt\,C}$, $\Delta n_{punt\,C}$).
The designator "c" to the names of the sources indicates *flags* (§3.4.5) and therefore these sources can be considered as potentially confused with interstellar emission. Their position, emission characteristics, or even existence may not be reliable.

Credit Marco Marongiu

IMAGING BACKGROUND:

- Software development and management for scientific data analysis (timing and imaging) and instrumentation simulation.

- Imaging science: gamma-ray (AGILE, Fermi), X-ray (XMM, Chandra), optical (ESO), radio (Medicina, SRT, JVLA).

- SRT, total-power, C-K bands, OTF maps (and timing).

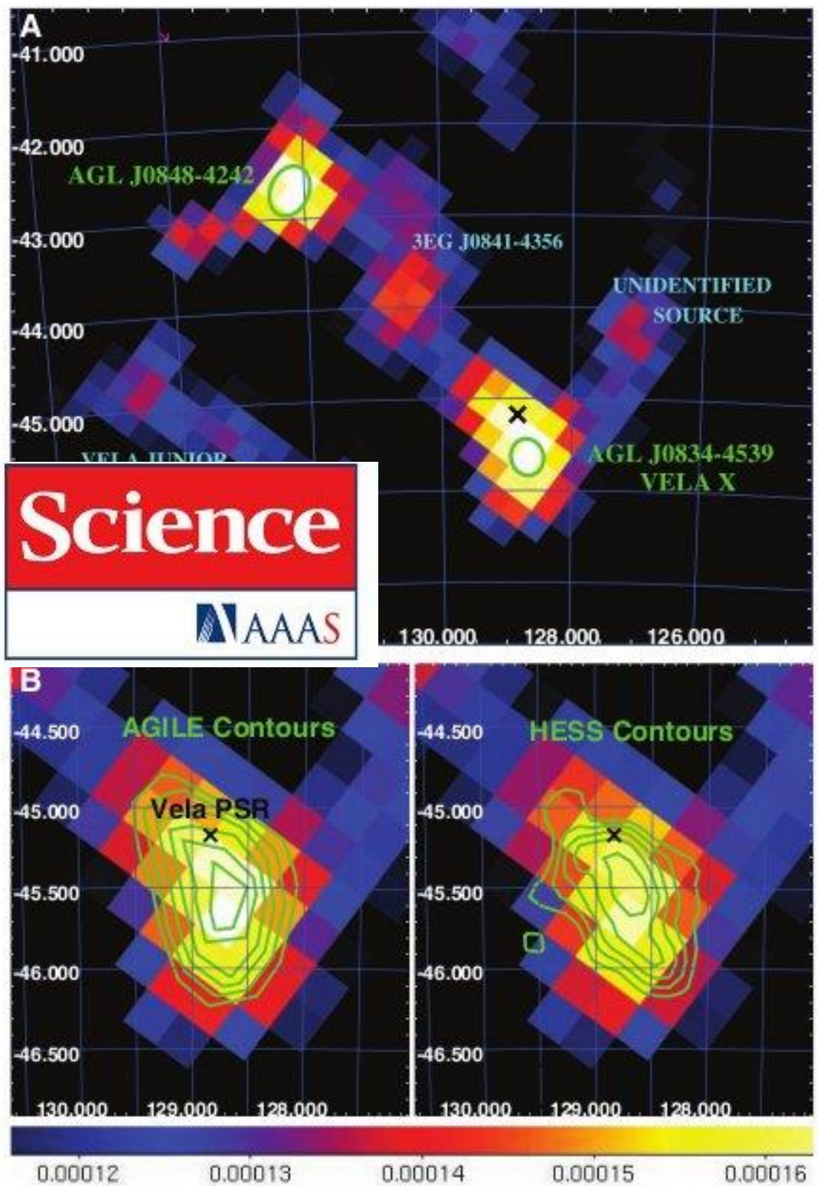

Pellizzoni et al., 2010
Pellizzoni et al., 2011

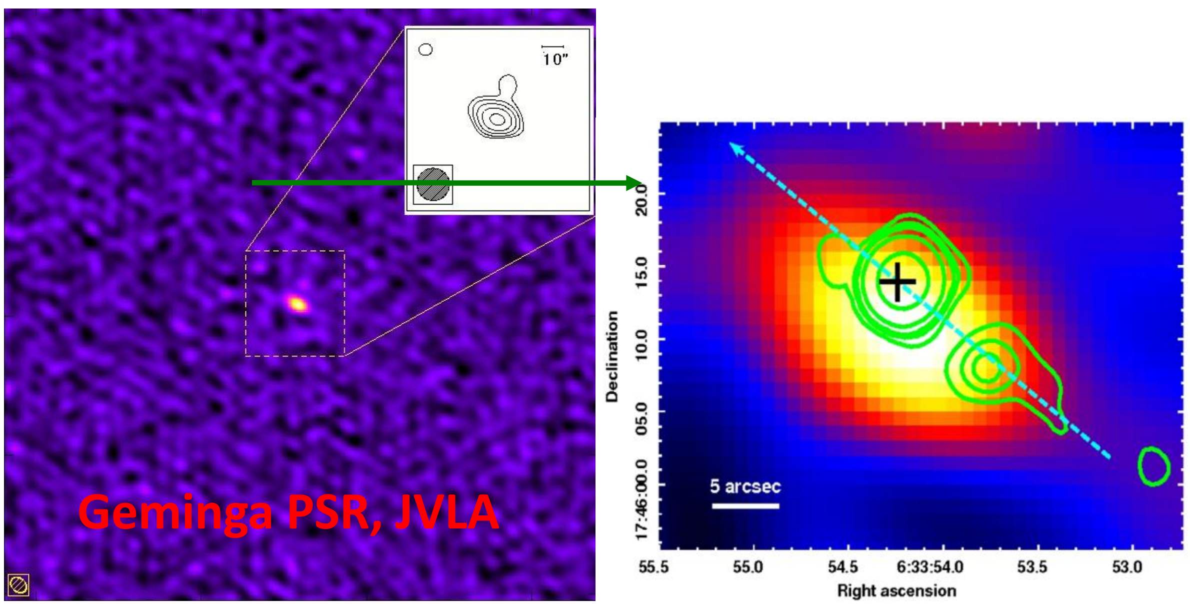

3C 58 with LOFAR

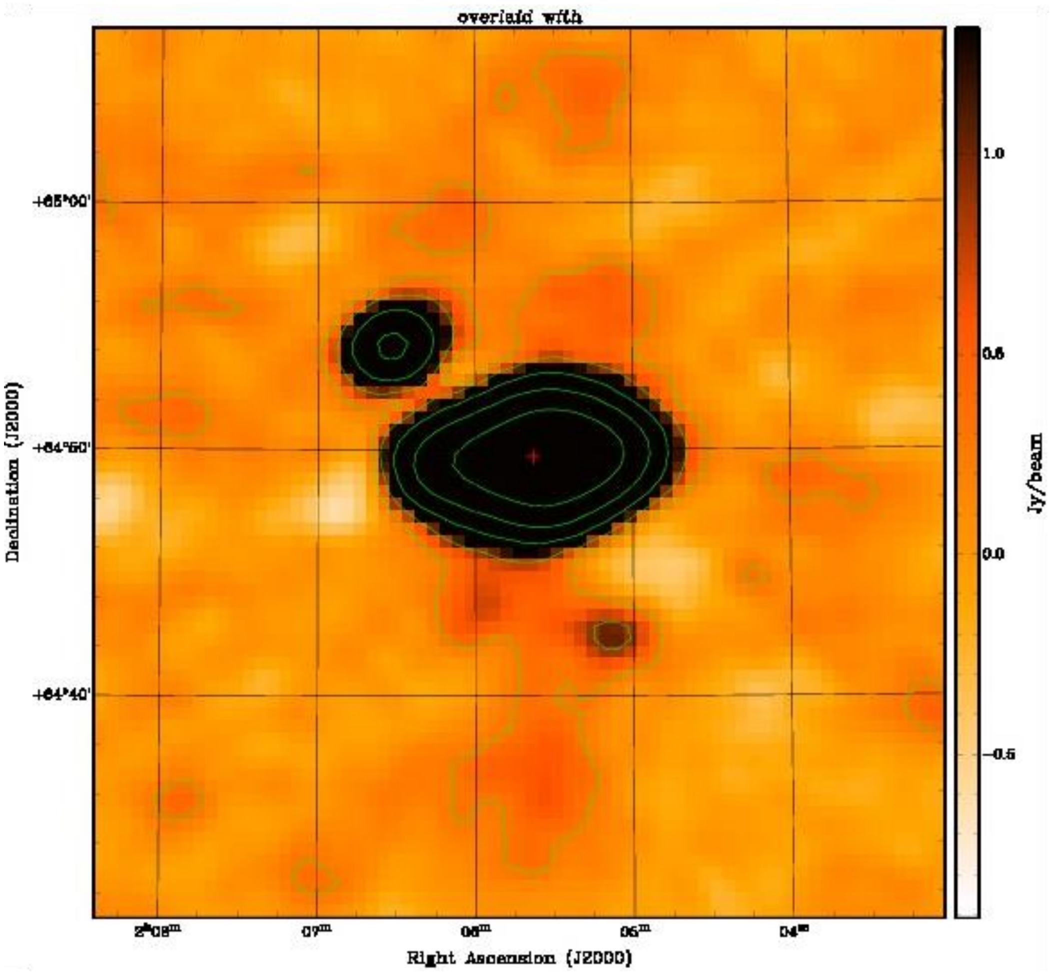

Pilia et al., in prep.

SNR 3C157:

32m Medicina + optical image

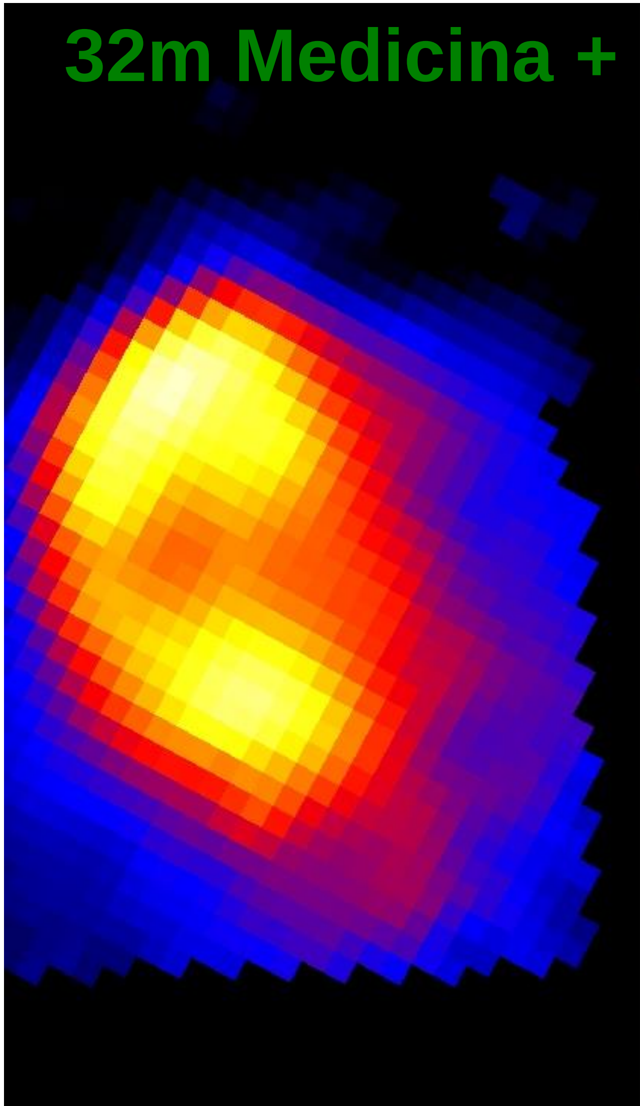

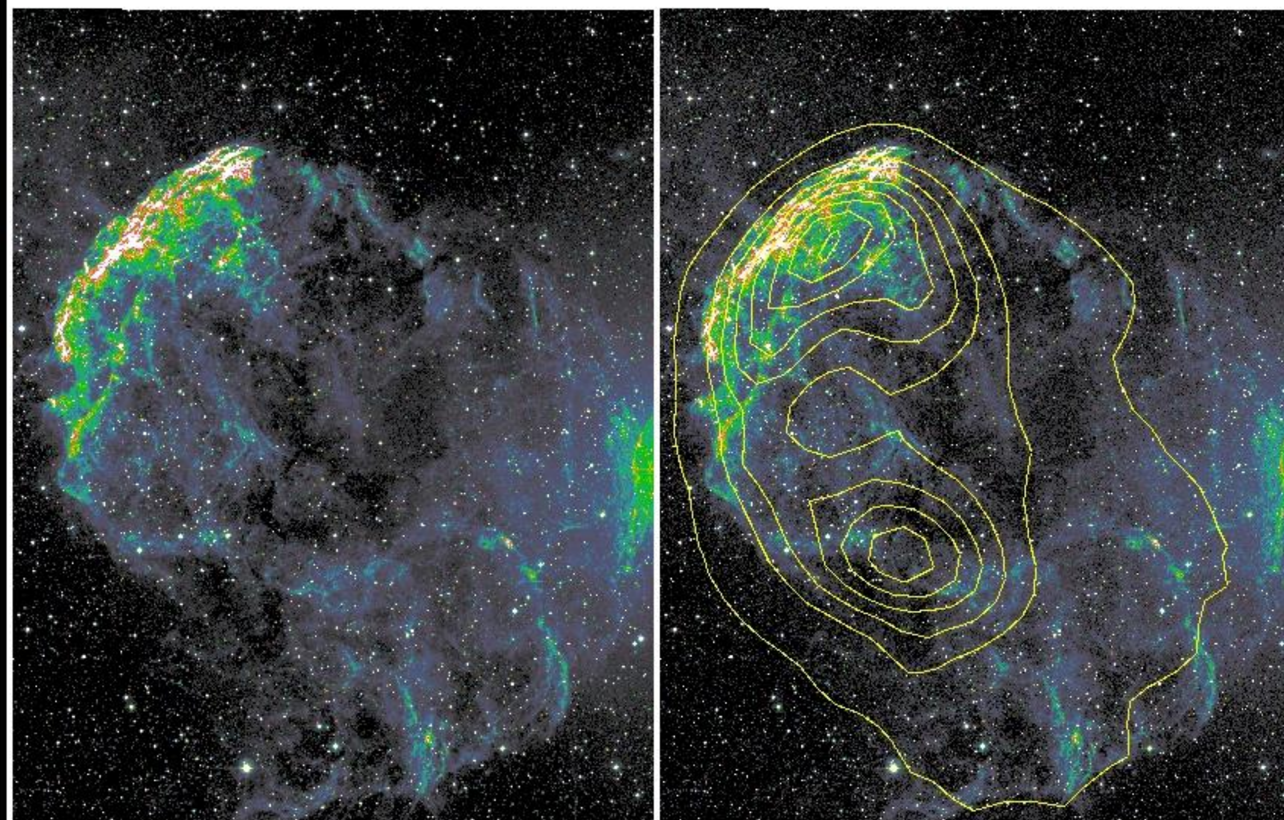

In collaboration with Giuliani, Righini et al.

Pulsar Wind Nebulae: Imaging with SRT

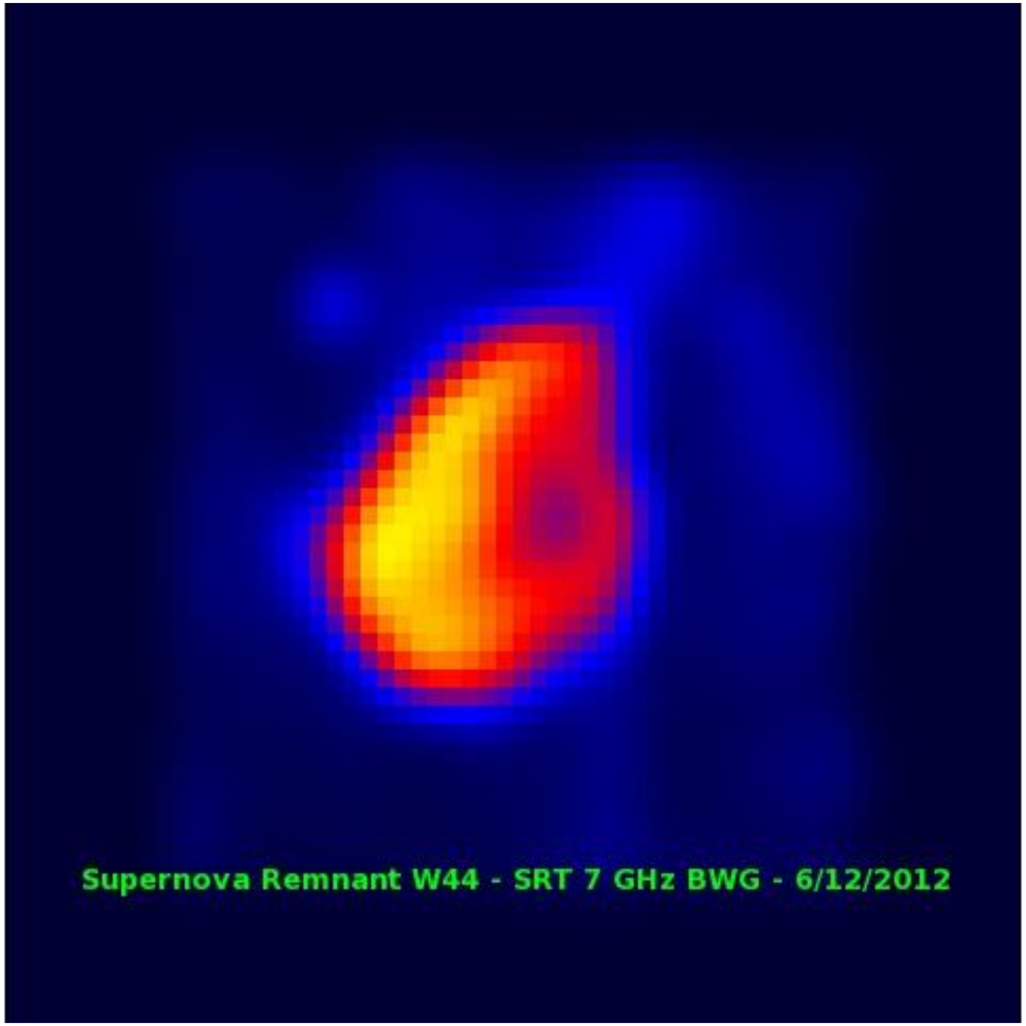

Early SDI applications: December 2012, SNR W44 at 7 GHz BWG, 1.5’ bin (**first resolved image of SRT**)

Credits:
Alberto Pellizzoni for the AV Team

Pulsar Wind Nebulae: Imaging with SRT

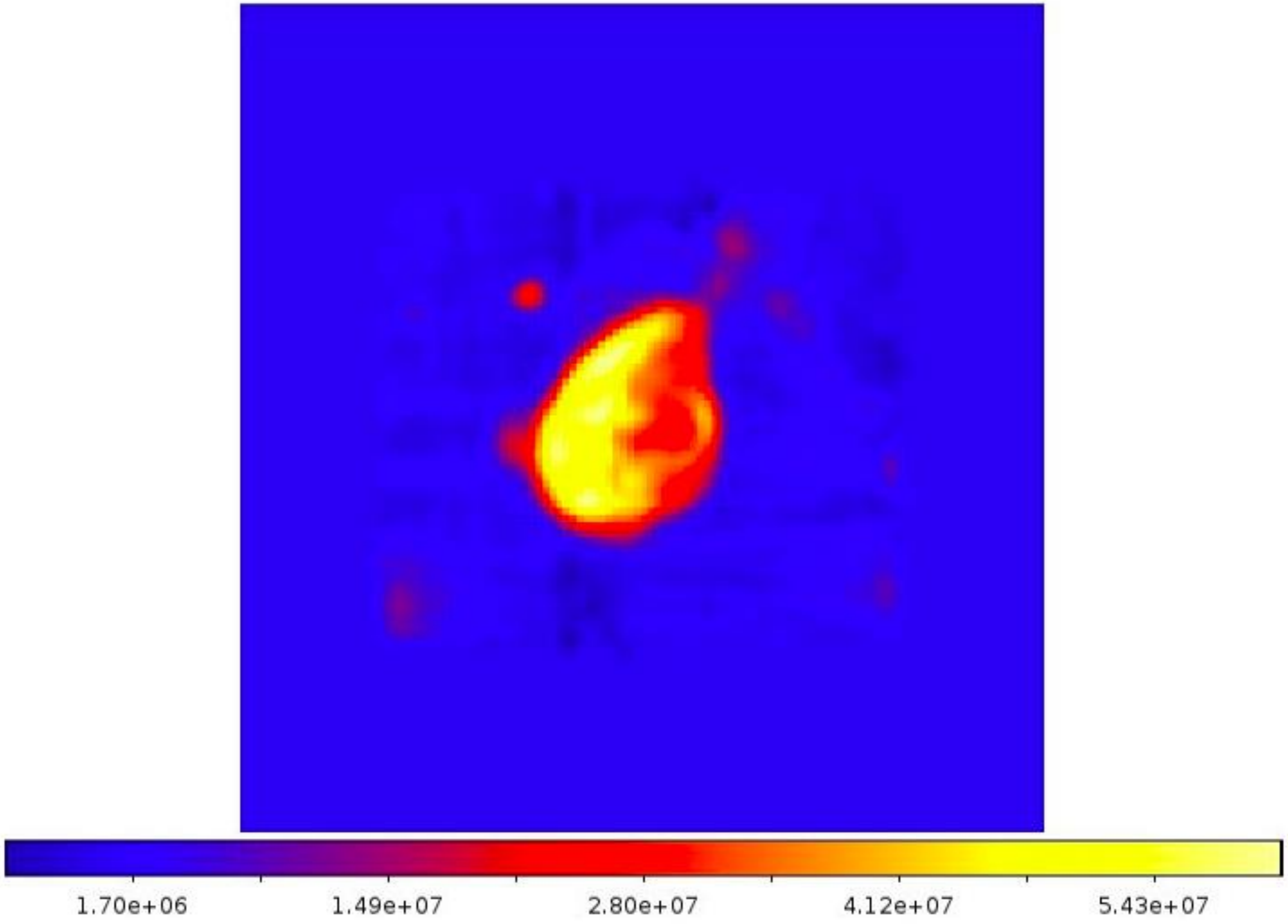

SNR W44 using ROACH 2 Boards.
C-band,
Bandwidth = 2048
# Channels = 2048
9 dumps/sec

Credits:
Melis, Concu, Trois for the AV Team

Summary and Conclusions

- Developement of a software tool for pulsar studies using a multi-telescope database
- Search for radio counterpart of pulsars, PWNe and unidentified gamma-ray sources
- Search for gamma-ray counterpart of pulsars and PWNe detected with SRT
- Providing a multi-wavelength pulsar database
- Understanding of pulsar emission mechanisms

Thank you!